PREDICTING AND ANALYZING MEMORIZATION WITHIN LLMS FINE-TUNED ~~LARGE LANGUAGE MODELS~~FOR CLASSIFICATION

Anonymous authors
Paper under double-blind review

ABSTRACT

Large Language Models have received significant attention due to their abilities to solve a wide range of complex tasks. However these models memorize a significant proportion of their training data, posing a serious threat when disclosed at inference time. To mitigate this unintended memorization, it is crucial to understand what elements are memorized and why. Most existing works provide *a posteriori* explanations, which has a limited interest in practice. To address this gap, we propose a new approach ~~based on sliced mutual information~~ to detect memorized samples *a priori* ~~, in a classification setting~~in LLMs fine-tuned on classification tasks. It is efficient from the early stages of training ~~, and is~~ and readily adaptable to ~~practical scenarios~~other classification settings, such as training vision models from scratch. Our method is supported by new theoretical results that we demonstrate, and requires a low computational budget. We obtain strong empirical results, paving the way for systematic inspection and protection of these vulnerable samples before memorization happens.

1 INTRODUCTION

Large Language Models (~~LLM~~LLMs) have revolutionized the way we approach natural language understanding. The availability to the general public of models such as ChatGPT, capable of solving a wide range of tasks without adaptation, has democratized their use. However, a growing number of ~~articles~~ publications have shown that these models memorize a significant proportion of their training data, raising some legal and ethical challenges (Zhang et al., 2017; Carlini et al., 2023; Mireshghallah et al., 2022b). The impact of memorization is ambiguous. On the one hand, it poses a serious threat to privacy and intellectual property because ~~LLM~~ LLMs are often trained on large datasets including sensitive and private information. Practical attacks have been developed to extract this information from training datasets (Carlini et al., 2021; Lukas et al., 2023; Yu et al., 2023; Nasr et al., 2023), and ~~LLM~~ LLMs have also been shown to plagiarize copyrighted content at inference time (Lee et al., 2023; Henderson et al., 2024). On the other hand, memorization has a positive impact on model's performance, because memorized samples are very informative. Studies revealed that outliers are more likely to be memorized, and that these memorized outliers help the model to ~~generalized~~ generalize to similar inputs (Feldman, 2020; Feldman & Zhang, 2020; Wang et al., 2024).

Mitigating the negative impacts of memorization while still harnessing its advantages is a challenging task, that requires varying approaches based on the sensitivity of the training data and the purpose of the model. However, it is hard for practitioners to evaluate the potential risk of memorized samples, because empirical defenses often fail to capture the most vulnerable samples from the training set (Aerni et al., 2024). To address this gap, we propose a new method to audit models under development and predict, from the early stages of training, the elements of the training data that the LLM is likely to memorize. Our first goal is to provide an efficient tool for practitioners to inspect vulnerable elements ~~before they are memorized in a classification setting, and implement context-appropriate mitigation techniques~~and chose an appropriate mitigation strategy: anonymization, differential privacy, ~~removal~~accepting the risk, etc.

~~Our method uses *Pointwise Sliced Mutual Information (PSMI)* (Goldfeld & Greenewald, 2021; Wongso et al., 2023a) at the first stages of~~ Our second goal is to enable researchers to design new empirical defenses that optimally allocate their privacy budgets to protect the most vulnerable samples, leading to a better privacy-utility trade-off. For both goals, it is crucial to predict memorization early in the training pipeline and at minimal cost. Indeed, *a-posteriori* measures of memorization, such as LiRA (Carlini et al., 2022a) or counterfactual memorization (Feldman & Zhang, 2020), require not only the completion of the training of the model, but also the training of several *shadow models*. This is extremely computationally expensive, and practitioners typically cannot afford it. On the other hand, for researcher developing empirical defenses, it is crucial to detect vulnerable samples as soon as possible to protect them before they are memorized. Our method achieves this by predicting memorization after only 2% to 5% of the training steps, without requiring any shadow model.

To predict memorization before it occurs, we interrupts training ~~to predict memorization (see figure 1). We interrupt training~~ when the median training loss has significantly decreased, typically by 95% (see Figure 1). This indicates the model has ~~learnt~~ learned simple patterns in the hidden representation, enabling it to accurately classify the majority of ~~typical~~ samples, without resorting to memorization. At ~~that~~ this stage, we measure ~~PSMI~~ the consistency between the labels and the hidden representation of the elements within the partially trained model. ~~PSMI is a statistical measure of how *surprising* the joint realization of two data distributions is. If an element has a negative PSMI~~If a hidden representations is unable to adequately explain its assigned label, it indicates that ~~it~~ the data sample behaves like a local outlier, within the data distribution's long tail (Zhu et al., 2014). ~~Its hidden representation is unable to adequately explain its assigned label.~~ Such outliers are particularly vulnerable to memorization, because the model will likely fail to learn meaningful representations for them, and will instead simply memorize them (Feldman & Zhang, 2020). ~~Based on this observation, we anticipate that elements with a negative PSMI at this stage of training will likely be memorized in the subsequent epochs. This intuition is supported by theoretical results and strong empirical evidences (see sections 2.2 and 3).~~

~~We predict memorization when the median training losshas decreased by 95%. This happens quite early in the training pipeline, typically after only 2% to 5% of the training steps. This is a key difference from Feldman & Zhang (2020), Zhang et al. (2023), or Leemann et al. (2024), who explain memorization *a posteriori* by correlating it with cross-influence, prediction simplicity, or test loss of a fully trained model, among others. All these methods require to fully train one or more *shadow model*, which is computationally expensive. Conversely, our metric only requires one forward pass per sample, which is considerably less.~~ We evaluated four approaches to quantify the consistency between the hidden representation and the label, with the objetive to predict memorization in the fully trained model : loss, logit gap, Mahalanobis distance (Mahalanobis, 1936), and Pointwise Sliced Mutual Information (PSMI) (Goldfeld & Greenewald, 2021; Wongso et al., 2023a). Except Mahalanobis distance, all approaches obtained strong empirical results. The loss is straightforward to implement and fast to compute, but requires an additional hyperparameter to define a threshold to separate elements that are predicted to memorized. The logit gap has no advantage over the loss. On the other hand, PSMI saves one hyperparameter because we demonstrated that zero is a natural threshold to use. However, it marginally increases the computation cost and is more complicated to implement.

To the best of our knowledge, ~~(Biderman et al., 2023)~~ Biderman et al. (2023) is the only ~~other practical approach to predict memorization~~ baseline to which our approach can be compared. It predicts memorization in LLMs trained on generative tasks, with a reasonable computational budget and *before* the end of training~~and with a reasonable computational budget. It is particularly useful for practitioners who wish to evaluate modelsduring the development phase. Their technique, leveraging early memorization , was pioneer, and they obtained a~~ . However, memorization is defined differently for generative and discriminative tasks. They use *k-extractability* (Carlini et al., 2021) , which is very cheap to compute for generative models, but not applicable to classification models. For these models, memorization is often defined as vulnerability to membership inference attack (Shokri et al., 2017), which is much more expensive to compute. Our approach is only applicable to classification models, for which we did not find any comparable baseline. This is why we adapted the method of Biderman et al. (2023) to a classification setting, even though its computational cost becomes prohibitive due to the increase of the cost of measuring memorization (see Appendix C.1). Despite this adaptation, we observed similar results: at the early stages of training, a low False

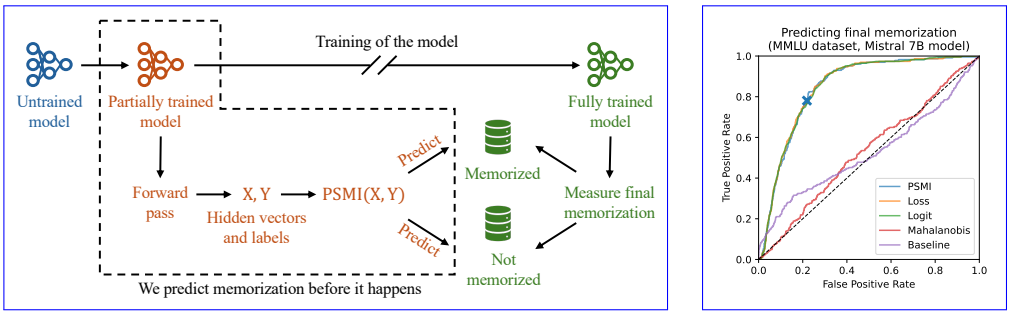

(a) We predict memorization from the early stages of training (b) Performance of the prediction

Figure 1: Figure 1a: We interrupt training when the median training loss has decreased by 95%. We compute a forward pass to retrieve X, the hidden representation of the inputs within the partially trained model. We measure the consistency between X and the label Y, and use it to predict memorization within the fully trained model. Figure 1b: Evaluation of the four metrics we used to quantify the consistency between X and Y: PSMI, loss, logit gap, and Mahalanobis distance. "Early memo" is our baseline, adapted from Biderman et al. (2023) (see Appendix C.1). The cross represents the default threshold for PSMI, equal to zero (see Algorithm 1 and Theorem 1).

Positive Rate (FPR) ~~in a pre-training setting. However, their~~ can be achieved, but not a high True Positive Rate (TPR)~~was low~~, because vulnerable samples ~~are not memorized yet at the early stages of training~~have not yet been memorized. Conversely, our approach obtains both high TPR and low FPR, paving the way for inspecting and protecting vulnerable samples under realistic conditions.

~~**Our main contributions can be summarized as follows.**~~

Our main contributions can be summarized as follows.

- We ~~propose a new approach based on PSMI~~ demonstrate that it is possible to predict, from the early stages of training, if a sample will be memorized when fine-tuning a LLM for a classification task ;
- We formalize the threat model ~~involved when predicting memorization~~ and propose FPR at high TPR as the ~~standard evaluation metric for subsequent work in that domain~~ evaluation metric ;
- We ~~demonstrate theoretical results to justify the use of PSMI to predict memorization~~ compare several metrics and discuss their respective advantages ;
- We validate the effectiveness of our approach for three different 7B ~~models and~~ LLMs fine-tuned on three different multi-choice question datasets ~~, and use our results to analyze the dynamics of memorization during the fine-tuning of a LLM~~ ;
- We ~~provide default hyperparameters to make our method readily adaptable to other settings~~demonstrate its adaptability by applying it as-is to vision models trained from scratch.

~~We predict memorization from the early stages of training~~ ~~Performance of the prediction~~ ~~Subfigure 1a: We interrupt training when the median training loss has decreased by 95%. Then, we compute a forward pass to retrieve the hidden representation of the inputs within the partially trained model. Then, we estimate Pointwise Sliced Mutual Information (PSMI) between these vectors and the labels, and use it to predict memorization within the fully trained model. Subfigure 1b: We compute PSMI at the last layer of the model, and predict that samples with negative PSMI will be memorized in the subsequent epochs (see algorithm 1). This leads to strong results (in green). In orange, we optimize the layer used for the PSMI and the threshold applied on it to improve the TPR/FPR trade-off. In blue, we use "early memorization" as a predictor, with near-random results, showing that samples are not memorized yet when we evaluate our metric.~~

1.1 Related work

Membership Inference Attacks (MIA) ~~Membership Inference Attacks~~ These attacks were first introduced by Shokri et al. (2017), and aim to determine whether a target individual element was part of a target model's training set. Although they are less realistic and practical than extraction attacks (Carlini et al., 2021; Lukas et al., 2023; Nasr et al., 2023), membership inference attacks have become the standard approach for measuring the amount of private information a model can leak. Popular attacks such as the ones of Shokri et al. (2017); Carlini et al. (2022a); Wen et al. (2023) involve training a great number of *shadow models* with different training data. Due to the significant computational resources required, alternative attack methods have been developed that necessitate training fewer shadow models or none at all (Yeom et al., 2018; Mattern et al., 2023; Zarifzadeh et al., 2024).

Several definitions of unintended memorization in neural networks ~~First, memorization can be~~ For discriminative models, memorization is usually defined as vulnerability to ~~membership inference attacks~~MIA, as in ~~(Mireshghallah et al., 2022b; Carlini et al., 2022b; Meeus et al., 2024) . Second, to~~ (Mireshghallah et al., 2022a; Carlini et al., 2022b; Aerni et al., 2024). Counterfactual memorization can also be applied to such models, requiring training multiple models with varying datasets to capture the influence of individual data samples (Feldman & Zhang, 2020) . On the opposite, to focus on more realistic threats, ~~some papers defined memorization~~ memorization can be defined as vulnerability to extraction or reconstruction attacks (Carlini et al., 2018; 2021; 2023; Biderman et al., 2023; Lukas et al., 2023; Dentan et al., 2024). ~~However, as~~ These definitions are mostly used with generative models, as such attacks are more complex to implement on discriminative models and often achieve lower performance. As pointed out by Lee et al. (2022); Prashanth et al. (2024), a large majority of elements extracted ~~with these attacks~~ consist of common strings frequently repeated in standard datasets. ~~To take duplication into account, counterfactual memorization , was introduced (Feldman & Zhang, 2020; Zhang et al., 2023). It involves training several models with different training datasets, to capture the actual influence of each individual point on a model. This definition was extended to self-supervised learning by Wang et al. (2024). A very computationally-efficient~~

variant was proposed by Lesci et al. (2024). This is why counterfactual memorization was adapted to generative models (Zhang et al., 2023; Wang et al., 2024; Pappu et al., 2024; Lesci et al., 2024). Finally, MIA can also be used for generative models (Meeus et al., 2024).

Explaining and predicting memorization In machine learning, memorization has been commonly associated with overfitting and considered the opposite of generalization. However, this belief was challenged by Zhang et al. (2017), who proved that a model can simultaneously perfectly memorize fit random labels and achieve state-of-the-art generalizationreal samples. This phenomenon was studied further by Arpit et al. (2017); Chatterjee (2018), followed by Feldman (2020) who provided a theoretical framework to explain how memorization can in fact increase generalization. His idea is that a substantial number of elements in typical datasets belong to the long tail of the distribution (Zhu et al., 2014), meaning that they behave like local outliers, unrepresentative of the overall distribution. As a result, memorizing them helps the model to generalize to similar samples at inference time. This idea was confirmed empirically by Feldman & Zhang (2020), and later by Zhang et al. (2023), who observed that memorized samples are relatively difficult for the model. Similarly, Wang et al. (2024) observed that memorization in self-supervised learning can increase generalization.

A different approach to explain memorization is to analyse the hidden representations learnt by the model. For example, Azize & Basu (2024) linked the privacy leakage of a sample to the Mahalanobis distance (Mahalanobis, 1936) between the sample and its data distribution. Leemann et al. (2024) evaluated several metrics to predict memorization from a reference model, and concluded that the test loss is the best predictor. Wongso et al. (2023b) computed Sliced Mutual Information (Goldfeld & Greenewald, 2021) between the hidden representations and the labels. They explain theoretically why a low SMI indicates memorization, and successfully observed this in practice.

These approaches provide *a posteriori* explanations of memorization, because they are either computed from the fully trained model or from a reference model. On the opposite, Biderman et al. (2023) introduced a new method to predict memorization *before* the end of pre-training. They obtain promising results and great accuracy. However, they get low recall scores, indicating that a significant proportion of the samples that are memorized by the final model could not be detected using their metrics. As they acknowledge, this is an important shortcoming of their method.

1.2 THREAT MODELPROBLEM SETTING

We consider a threat model similar to that of Biderman et al. (2023), applied to fine-tuning rather than pre-training]Predicting Threat model: predicting memorization, not mitigating it

We consider a threat model similar to that of Biderman et al. (2023), applied to fine-tuning rather than pre-training We adapt the setting of Biderman et al. (2023). We assume that an engineer is planning to fine-tune a LLM on a private dataset for a classification task, and that a small proportion of this dataset contains sensitive information that should not be memorized by the model for privacy concerns. The engineer wishes to has full access to the model, its training pipeline and intermediate checkpoints. They do not have the computational budget to train the shadow models needed for *a posteriori* measures of memorization such as LiRA or counterfactual memorization (see Section 1.1). Consequently, they wish to perform some tests with a low computational budget at the beginning of the full training run ,with the objective to predict approximate *a posteriori* memorization, and determine if the sensitive samples will be memorized by the fully trained model (see figure Figure 1). They have full access to the model, its training pipeline and intermediate checkpoints, and wish to

The engineer wishes to dedicate only a small amount of compute for these tests. Depending on the results of the tests and the context of the model, the engineer would then evaluate the privacy risks, and take decisions : accept the risk, or abort training and change the architecture, or , to reduce the overhead of confidentiality checks. Moreover, they aim to detect vulnerable samples early to inspect them before they are memorized and decide whether to accept the privacy risk, anonymize or remove some the samples, or implement mitigation techniques, etc. This is particularly important for researchers developing some empirical defense that optimally allocate their privacy budgets to protect the most vulnerable samples without altering non-vulnerable samples, leading to a better privacy-utility trade-off. We do not make any assumption on these subsequent decisions

the subsequent decisions made by the engineer, and only focus on developing a good predictor of which ~~element~~ elements will be memorized by the final model. ~~Indeed, there are reasons to keep memorized samples in the training set. These samples can often help the model to generalize (Feldman & Zhang, 2020; Wang et al., 2024). Also, due to the Privacy Onion Effect, non-sensitive memorized samples can act as a protective layer preventing sensitive samples from being memorized (Carlini et al., 2022b). Conversely, some sensitive samples such as copyrighted content are desirable in the training set to achieve high level performance, but undesirable to memorize (Min et al., 2023; Henderson et al., 2024).~~

Evaluation metrics: FPR at high TPR We use the prediction based on the partially trained model to predict memorization in the fully trained model. As for membership inference attacks, we evaluate the True Positive Rate / False Positive Rate (TPR / FPR) trade-off in the prediction (Carlini et al., 2022a). The TPR represents the proportion of memorized samples in the final model which are correctly detected based on the partially trained one, and the FPR represents the proportion of non-memorized samples which are wrongly detected. We prefer TPR / FPR to precision / recall because it is independent of the prevalence of memorized samples. However, as noted by Biderman et al. (2023), a high TPR is more important than a low FPR. Indeed, false positives lead the engineer to be overly cautious, which is unprofitable, but does not threaten privacy. Conversely, false negatives lead the engineer to underestimate memorization, which entails a privacy risk. As a consequence, we will ~~evaluate FPRat a fixed high TPRvalue, such as~~ focus on regions of the FPR/TPR curves that achieve a high TPR, typically greater than 75~~%. We propose to use this "FPR at high TPR" as a standard evaluation metric for subsequent work related to predicting memorization~~%. The Area Under the Curve (AUC) can be used to compare metrics with a single numerical value, although it presents a simplistic view of the TPR/FPR trade-off.

Experimental settings Most studies on memorization in a classification setting focus on models of intermediate size trained on datasets such as CIFAR-10 or CIFAR-100 (Aerni et al., 2024; Carlini et al., 2022b; Feldman & Zhang, 2020). We have decided to consider more recent scenarios using LLMs fine-tuned on classification tasks. Indeed, generative models are increasingly trained to produce formatted outputs for tasks previously handled by discriminative models, such as information extraction (Kim et al., 2022; Dhouib et al., 2023), sentiment analysis (Šmíd et al., 2024), or recommendation (Geng et al., 2022; Cui et al., 2022). Moreover, privacy is often a significant concern for fine-tuning, as the datasets used for this purpose frequently contain sensitive private information.

Although our experiments focus on fine-tuned LLMs, our method relies on the specific properties of neither LLMs nor fine-tuning. Consequently, our method is suitable for any model trained for classification tasks. In Section 3.2, we apply our method as-is to a Wide Residual Network (Zagoruyko & Komodakis, 2016) trained from scratch on CIFAR-10, yielding conclusive results.

For most experiments, we used three pretrained models with similar architectures: Mistral 7B v1 (Jiang et al., 2023), Llama 7B v2 (Touvron et al., 2023), and Gemma 7B (Team et al., 2024). We used three popular academic benchmarks: MMLU (Hendrycks et al., 2021b), ETHICS (Hendrycks et al., 2021a) and ARC (Boratko et al., 2018). We fine-tuned these models using LoRA (Hu et al., 2022) and question-answering templates asking the model to output the label. Models are trained using Next Token Prediction task, computing the loss only for the token corresponding to the label.

2 Methodology

2.1 Preliminary

Hidden representations in Large Language Models We consider a decoder-only transformer-based LLM such as Llama 2 7B (Touvron et al., 2023) trained on a multi-choice question (MCQ) dataset such as MMLU (Hendrycks et al., 2021b). With this type of architecture, all tokens of the input are embedded into *hidden representations* in $\mathbb{R}^d$. They are successively transformed at each of the K layers to incorporate information from the context. For example, Llama 2 uses $d = 4096$ and $K = 32$. Finally, the representation of the last token at the last layer is used to predict the answer.

For $k \in [\![1, K]\!]$, let $X_k \in \mathbb{R}^d$ be the hidden representation of the last token after the k-th layer, and $Y \in \{0, 1, 2, \dots, r\}$ the answer of the MCQ. We can think of X_k and Y as random variables following a joint probability distribution $\mathcal{D}_k$ that can be estimated from the dataset. In the following, we use information-theoretic tools to analyze the interplay between variables X_k and Y. Note that $\mathcal{D}_k$ and X_k depend of the training step, but we omit this aspect in our notations to consider a LLM that we freeze to analyze its representations.

(Pointwise) Sliced Mutual Information Sliced Mutual Information (SMI) was introduced by Goldfeld & Greenewald (2021). Similar to Shannon's Mutual Information (denoted I), it measures the statistical dependence between two random variables such as X_k and Y. Intuitively, it measures how much the realization of X_k tells us about the realization of Y. If they are independent, the mutual information is ~~null~~ zero ; and if X_k fully determines Y, the mutual information is maximal. In our setting, it represents how useful the hidden representations are to predict the labels. Thus, we expect the SMI to increase with k as the representations become more efficient over layers. Indeed, SMI is not subject to the data processing inequality, contrary to I (Goldfeld & Greenewald, 2021).

Definition 1 *Sliced Mutual Information (*SMI*) is the expectation of Mutual Information (denoted* I*) over one-dimensional projections sampled uniformly at random on the unit sphere (denoted* $\mathcal{U}(\mathbb{S}^d)$*):*

$$\text{SMI}(X_k, Y) = \mathop{\mathbb{E}}_{\theta \sim \mathcal{U}(\mathbb{S}^d)} \left[\text{I}(\theta^T X_k, Y)\right] = \mathop{\mathbb{E}}_{\theta \sim \mathcal{U}(\mathbb{S}^d)} \left[\mathop{\mathbb{E}}_{(X_k, Y) \sim \mathcal{D}_k} \left[\log \frac{p(\theta^T X_k, Y)}{p(\theta^T X_k) p(Y)} \right] \right] \quad (1)$$

Pointwise Sliced Mutual Information (PSMI) was introduced by Wongso et al. (2023a) and used as an explainability tool. For every individual realization (x_k, y) of the variables (X_k, Y), it represents how surprising it is to observe x_k and y together. For example, a low PSMI means that label y was unexpected with representation x_k, maybe because all similar representations to x_k are associated with another $y' \neq y$ in the dataset.

Definition 2 *Pointwise Sliced Mutual Information (*PSMI*) is defined for every realization* $(x_k, y) \in \mathbb{R}^d \times [\![0; r]\!]$ *of the variables* (X_k, Y) *as:*

$$\text{PSMI}(x_k, y) = \mathop{\mathbb{E}}_{\theta \sim \mathcal{U}(\mathbb{S}^d)} \left[\log \frac{p(\theta^T x_k, y)}{p(\theta^T x_k) p(y)} \right] \quad (2)$$

Here, p represents the value of the probability distribution function. It depends on the joint distribution $\mathcal{D}_k$, and can be estimated numerically by approximating $p(\theta^T x_k \mid y)$ by a Gaussian (Wongso et al., 2023a). The resulting estimator of PSMI is very fast to compute and easy to parallelize. The bottleneck is to compute the hidden representations x_k, which requires one forward pass per sample.

2.2 Why elements with low PSMI are likely to be memorized

Intuitively, PSMI measures the dependency between the hidden representation of a data sample and its label. As a result, PSMI should be lower for outliers and points that are hard to classify. Following the results of Feldman & Zhang (2020), these are the points that are most likely to be memorized.

The following theorem validates this intuition. We consider a binary classification setting with balanced classes and some outliers. With probability $1 - \varepsilon$, the point is not an outlier, and the hidden representation X follows a Gaussian distribution (~~eq~~Eq. 3). This Gaussian behavior is a classical hypothesis derived from the central limit theorem applied to deep neural networks (Matthews et al., 2018). Conversely, with probability ε, the point is an outlier: X does not necessarily follow the Gaussian distributions, and Y is sampled uniformly at random (~~eq~~Eq. 4). We prove that on average PSMI is positive for non-outliers (~~eq~~Eq. 5), and ~~negative~~ zero for outliers (~~eq~~Eq. 6). See proof in ~~appendix~~ Appendix B.

Theorem 1 *Let* $(X, Y) \in \mathbb{R}^d \times \{0, 1\}$ *be random variables. We assume that* $p(Y = 0) = p(Y = 1) = 0.5$ *and that* X *is a continuous random variable. We also assume that there exist* $\mu_0, \mu_1 \in \mathbb{R}^d$ *with* $\mu_0 \neq \mu_1$*, and* $\Sigma_0, \Sigma_1 \in \mathbb{R}^{d \times d}$*, and a Bernoulli variable* $\Delta \sim \mathcal{B}(\varepsilon)$ *with* $\varepsilon \in]0, 1[$ *such that:*

$$p(X \mid Y = 0, \Delta = 0) \sim \mathcal{N}(\mu_0, \Sigma_0) \quad \text{and} \quad p(X \mid Y = 1, \Delta = 0) \sim \mathcal{N}(\mu_1, \Sigma_1) \tag{3}$$

$$\forall x \in \mathbb{R}^d, \quad p(Y = 0 \mid \Delta = 1, X = x) = p(Y = 1 \mid \Delta = 1, X = x) = 0.5 \tag{4}$$

Given this, we then have:

$$\mathop{\mathbb{E}}_{X,Y} [\text{PSMI}(X, Y) \mid \Delta = 0] > 0 \tag{5}$$

$$\mathop{\mathbb{E}}_{X,Y} [\text{PSMI}(X, Y) \mid \Delta = 1] \approx 0 \tag{6}$$

2.3 Our method

~~A default algorithm for practitioners~~ ~~Based on theorem~~ Based on Theorem 1, we propose ~~the following algorithm~~Algorithm 1 to predict memorization. The three ~~values~~ hyperparameters in bold performed well in every setting we evaluated. We interrupt training when the median training loss decreases by **95%**, as this metric remains stable even in the presence of outliers. We measure PSMI at the **last layer**, which is consistently informative, and use a threshold of **zero**, as supported by Theorem 1. These default values yielded conclusive results when used with CIFAR-10, for which they were not optimized (see ablation studies in Section 3.2). Consequently, these hyperparameters are likely suitable for practitioners auditing models in diverse classification settings. To facilitate the use of this method, we provide a PyPI package containing an automated estimator of PSMI.[1]

As noted in the introduction, using the loss instead of PSMI also produced convincing results. An alternative to Algorithm 1 is to replace lines 2-3 with a forward pass to retrieve the loss (see Algorithm 2). The implementation is simpler, but it requires the practitioner to select a threshold to separate samples predicted to be memorized, as there is no natural threshold like zero for the PSMI.

Algorithm 1 ~~Predicting~~ Using PSMI to predict memorization

1: Interrupt training when the median training loss has decreased by at least **95%**.
2: Compute a forward pass for every sample to retrieve the hidden vector after the **last layer**.
3: Use ~~algorithm~~ Algorithm 1 in (Wongso et al., 2023a) to estimate PSMI for every sample.
4: Predict that every sample with **PSMI** $\leq$ **0** will be memorized.

~~Hyperparameters default values and optimization~~ ~~Algorithm 1 involves three hyperparameters with default values for practitioners willing to audit models under realistic conditions. These values can be optimized to improve the performance of the predictor, which is interesting for a research purpose, to analyze and understand memorization . First, we use a *criterion* to decide when to interrupt training. By default, we detect when the median training loss has decreased by 95% because it is stable even in the presence of outliers, and it correctly represents if the model behaves correctly for typical samples (see section **??**). Second, a *layer* to retrieve the hidden representations and compute PSMI. By default, we use the last layer because it is always very informative (see section 3.2). Third, a *threshold* to apply to PSMI to separate samples predicted to be memorized from the others. By default, we use value 0 because it is supported by theorem 1 (see sections 2.2 and 3.1).~~

3 Experimental results

~~Ground truth memorization and computational gains~~ We evaluate the efficiency of predicting memorization from the early stages of training, using several metrics that quantify the consistency between the hidden representations and the assigned label: PSMI (Algorithm 1), loss, logit gap, and Mahalanobis distance (see Appendix C.3). We compare these predictors to the baseline of

[1] hidden_github_url_pypi_package_for_review

Biderman et al. (2023), which we adapted to our classification setting. Its computational cost is much higher, but it is the only comparable approach we are aware of (see Appendix C.1). We use five combinations of dataset/model: ARC/Mistral, ETHICS/Mistral, MMLU/Mistral, MMLU/Llama and MMLU/Gemma (see Section 1.2).

To evaluate our approach, we resume training and measure memorization at the end. To ensure a fair comparison between our experiments and prevent over-training, we always stop training after ~~10 epochs (see appendix D.1)~~1 epoch. As in (Carlini et al., 2022b; Mireshghallah et al., 2022b; Aerni et al., 2024), we use vulnerability to LiRA membership inference attack ~~(Carlini et al., 2022a)~~ as our ground truth memorization metric (see ~~appendix~~ Appendix A.1). This attack provides a numeric score for each sample, which is a likelihood ratio computed from a large number of *shadow models*. We always display the natural logarithm of LiRA, so a positive score indicates that the element was memorized. ~~We used 100 shadow model (see appendix A.1.1)~~Unless otherwise stated, memorized samples are defined as the ones with log-LiRA ≥ 4, which means LiRA ≥ 54.6.

Computational gains The bottleneck of ~~algorithm~~ Algorithm 1 is computing a forward pass for every sample, which costs as much as $1/3$ of epoch (Hobbhahn & Jsevillamol, 2021). Moreover, we typically compute our metric after only 0.2 to 0.4 epochs (see ~~section~~ Section 3.2). Thus, our method costs about as much as $2/3$ of epoch. On the opposite, our ground truth memorization requires training 100 models for ~~10~~ 1 epochs, which is ~~1500~~ 150 times more expensive. ~~Using counterfactual simplicity is as expensive as our ground truth (Zhang et al., 2023). Less costly techniques such as the one of (Leemann et al., 2024) still require to fully train one reference model, which is 15 times more expensive than our approach. As a result, in addition to its theoretical justifications and its great adaptability (see last paragraph of section 3.1), our approach is considerably less expensive than *a posteriori* explanations of memorization.~~

~~**Experimental settings** We used three pretrained models of similar architecture: Mistral 7B v1 (Jiang et al., 2023), Llama 7B v2 (Touvron et al., 2023), and Gemma 7B (Team et al., 2024) . We used LoRA (Hu et al., 2022) to fine-tune these models because it is widely used by practitioners , making~~ As explained in Section 1.2, practitioners within our threat model ~~more realistic. We used three popular academic benchmarks : MMLU (Hendrycks et al., 2021b), ETHICS (Hendrycks et al., 2021a) and ARC (Boratko et al., 2018). They contain multi-choice questions, that we formatted with different templates to ask the model to predict the label. Due to the significant computational costassociated with LiRA's shadow models, we focused on five configurations: ARC/Mistral, ETHICS/Mistral, MMLU/Mistral, MMLU/Llama, and MMLU/Gemma.~~ do not have the budgets to compute such *a posteriori* measures of memorization. Our approach enables them to approximate memorization at minimal cost.

We used a HPC cluster with Nvidia A100 80G GPUs and Intel Xeon 6248 ~~40 cores CPUs. The training took between 3~~ 40-cores CPUs. The total computational cost of our experiments is 10961 GPU hours and ~~10 hours per model on a single GPU. Overall, our experiments are equivalent to around 5000 hours of single GPU and 4000 hours of~~ 5787 single-core CPU hours. This represents 0.57 tCO_2eq for this cluster (see `hidden_hpc_url_for_review`).

3.1 ~~Dynamics of memorization~~

~~Dynamics of PSMI (layer 20) Dynamics of memorization Dynamics of the loss Three phases of training (here, for MMLU/Llama). The first vertical line (epoch 0.4) represents the moment when the median loss has decreased by 95%. The second one (epoch 5) represents the best validation accuracy. Orange and blue represent "difficult" (PSMI < 0 at epoch 0.4) and "easy" samples (PSMI > 0 at epoch 0.4), respectively. For each of them, the solid line is the median, and the shaded area represents 25%-75% quantiles. Up to the first line we have **pattern initialization**, where the model learns simple pattern to correctly classify easy samples. Then, up to the second line, we have **pattern complexification**, where the model refines its patterns to accurately predict difficult samples. Finally, we have **pattern degeneration**, where representations become inefficient due to their too high complexity. Difficult samples are memorized during the last two phases, but it can be detected by analyzing PSMI at the end of pattern initialization.~~

~~We observed that the learning process can be roughly divided into three phases (see vertical bars in figure **??**). In the following, we call *pattern* a statistical dependence within the hidden~~

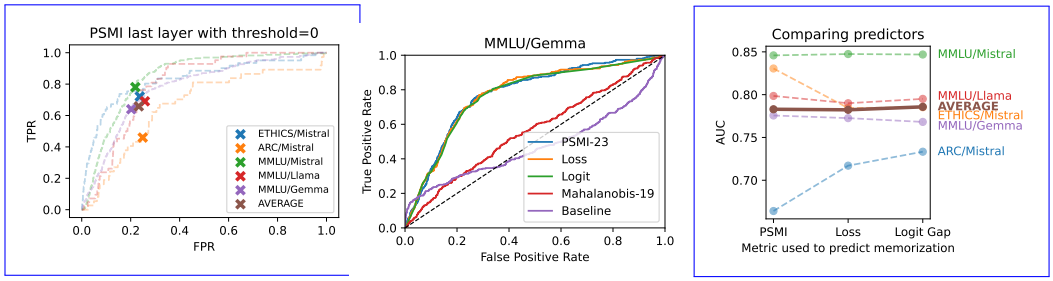

(a) Default performance (b) TPR/FPR trade-offs (c) Comparing predictors

Figure 2: ~~Default~~ Figure 2a: TPR/FPR trade-off of PSMI using the default hyperparameters of Algorithm 1 (crosses) compared to the trade-offs that can be obtained with the best layer (dashed lines). The prediction is computed when the median training loss has decreased by 95%. Figure 2b: Our baseline and Mahalanobis distance have near-random performance, whereas PSMI, loss, and logit gap are good predictors. "23" and "19" denote the layers used for computation, which perform best in these settings. Figure 2c: Comparing the AUC of the best predictors.

~~Subfigure 2b: The Mahalanobis distance (layer 13) and early memorization have near-random performance, whereas the PSMI (layer 29), the Loss, and the Logit gap are good predictors. Subfigure 2c: Evaluation of the three best predictors for each of our 5 settings. PSMI is more effective than the loss or the logit gap. Subfigure 2a: TPR and FPR scores of the default method and hyperparameters presented in algorithm 1 (crosses) compared to the TPR/FPR trade-off that can be obtained with the best layer (dashed lines). The prediction is computed at the first checkpoint where the median loss has decreased by 95%, using the layer with the best TPR@FPR=0.75 performance (except for the crosses in subfigure 2a which implement algorithm 1 and use the last layer).~~

~~representations that enables the model to perform its task. The superposition of all patterns learnt by the model results in the decision boundary that separates samples that are classified in each class. We call the first one **pattern initialization**. The model learns simple patterns, which are efficient to perform the task approximately. The median training and testing losses decrease quickly, because these patterns are sufficient to classify the majority of samples. However, there remains a population of difficult samples, belonging to the long tail of the data distribution, for which the training loss remains high. At this stage, memorization is negligible. Then, the second phase is **pattern complexification**. The model refines its patterns to improve its predictions on difficult samples, which significantly decreases their loss. The test loss also decreases and the test accuracy increases at first. However, as patterns become more and more complex, the test loss starts increasing while the test accuracy is still increasing. This is because these increasingly complex patterns bring easy elements closer to the decision boundary (which increases the test loss), but are still useful to generalize on difficult samples (which increases the test accuracy). During this phase, memorization progressively grows. Finally, the last phase is **pattern degeneration**. The model overfits its training data. The train loss, which was already low for both easy and hard train samples, gets even lower. The test loss increases, as well as memorization, especially for hard samples, and the test accuracy decreases. Moreover, PSMI decreases because the patterns become too complex to accurately explain the labels.~~

~~Using the criterion of measuring when the median training loss has decreased by 95% has been observed empirically to be a reliable indicator for tracking the end of pattern initialization. It is stable even in the presence of outliers, and as we see in figure **??**, it correctly marks a turning point where the PSMI starts to increase even for difficult samples. Samples that are difficult at that stage cannot be linked to the simple patterns learnt by the model, so they are likely to be difficult point for which the model will likely fail to learn meaningingful patterns and memorize them instead.~~

3.1 MEMORIZATION CAN BE RELIABLY PREDICTED~~USING PSMI~~

Our experiments demonstrate that memorization can be predicted accurately from the early stages of training~~(see figure 2). On average, the default hyperparameters presented in algorithm 1lead to a~~. In Figure 2a, we present the TPR and FPR values that are achieved with the procedure and the

default hyperparameters provided in Algorithm 1. On average, we obtained a **FPR of ~~15.3~~23.3%** and a **TPR of ~~88.7~~65.8%**. ~~This~~ These very good score proves that most memorized samples can be detected very early (high TPR) and with a great exactness (low FPR). ~~This shows a significant improvement compared to previous methods, like relying on early memorization, which was used by (Biderman et al., 2023) in a pre-training setting. See appendix C.3 for details on the predictors.~~

~~**TPR/FPR trade-off when optimizing the thresholds** In figure 2b, we vary the threshold used to separate samples we predict to be memorized. This results in the TPR/FPR trade-off that we plot in figure 2b. We compare PSMI with other predictors that appear in the literature: the loss of the training samples (Leemann et al., 2024), the logit gap (Carlini et al., 2022a), the Mahalanobis distance (Azize & Basu, 2024), and early memorization (Biderman et al., 2023) (see appendix C.3 for details). These last two methods proved ineffective. In figure 2c we perform a quantitative comparison by imposing a TPR objective of 75% and measuring the FPR we obtain. We observe that PSMI obtained better results in every setting, with an average of **FPR=7.3% @ TPR=75%**. This demonstrates that PSMI accurately captures susceptible samples from the early stages of training.~~

~~**TPR/FPR of the default algorithm** The TPR/FPR trade-offs presented above are interesting for a research purpose, but they cannot be implemented under realistic conditions. Indeed, practitioners do not have the computational budget to optimize the layer or the threshold set on the predictor. This is why we also evaluate the TPR and FPR obtained with the procedure and the default hyperparameters provided in algorithm 1. This yields a single TPR/FPR value for each setting, which we plot in figure 2a. The~~ The crosses corresponding to the default procedure are not exactly on the dashed lines of the same color. This is because the dashed lined are obtained by optimizing both the layer used to compute PSMI and the threshold used to separate samples that we predict to be memorized. The proximity of the crosses to the dashed lines indicates that the performance improvement gained from optimizing the layer is minimal (see ~~section~~ Section 3.2 for more details).

~~Why PSMI is~~ TPR/FPR trade-off when optimizing the ~~most practical estimator~~thresholds (Figures 2b and 2c) ~~PSMI has several advantages compared to other estimators. First, it yields slightly better FPR score than the loss or the logit gap. But most importantly, PSMI comes with a natural threshold~~

We vary the threshold used to separate samples we predict to be memorized~~. This threshold, equal to 0, is supported by theoretical results (see theorem 1), and obtains very good results in all our experiments. This is a significant difference from the loss or~~ , resulting in the TPR/FPR trade-off presented in Figure 2b. Our baseline and Mahalanobis distance proved ineffective. One the opposite, the FPR@TPR=75% is equal to 24.1% for PSMI, 24.6% for the loss and 23.1% for the logit gap, ~~for which a practitioner would have to tune an accurate threshold. This is why we assert that our approach is readily adaptable to predict memorization in every other classification setting.~~

~~We believe that the great adaptability of our method, combined with its theoretical justification and affordable computational cost makes it a very effective auditing tool for practitioners~~which demonstrates that a practitioner can detect the majority of memorized samples with an acceptable FPR. In Figure 2c we observe that PSMI, loss and logit gap perform similarly, and obtain a very high AUC value on average. This demonstrate that they accurately capture susceptible samples from the early stages of training. See Appendix D.1 for additional results.

3.2 Ablation studies

Impact of the timing of the measure (Figure 3) ~~We track the moment~~ In Algorithm 1, we predict memorization when the median training loss has decreased by 95%~~to detect the end of *pattern initialization* and predict memorization (see section ??)~~. To validate this choice empirically, we save the models every 0.2 epochs, and evaluate how efficiently memorization can be predicted at each checkpoint. As we observe in ~~figure~~ Figure 3a, the predictions start being effective only when the median training loss has decreased at lot, and the threshold of 95% proved to be effective in all our settings. We observe in Figure 3b that it corresponds to the moment where the PSMI of samples memorized by the final model is much lower than that of non-memorized samples. Indeed, the patterns learnt by the model before are not relevant enough for PSMI to accurately quantify if a sample will likely be hard to learn. ~~We obtained results similar to those shown in figure 3a for our five~~

~~experimental settings~~Importantly, as shown in Figure 3c, memorized samples are not yet memorized at that moment. This indicates that a practitioner within our threat model can implement mitigation techniques based on the privacy risks associated with memorized samples without restarting the training process. See Section 1.2 for details on our threat model and see Appendix D.1 for additional plots.

Impact of the ~~choice of ground-truth~~ memorization threshold (Figure 4a) ~~We use LiRA to define the ground-truth memorization that we predict with PSMI. We use a threshold to split samples that should be predicted as "memorized" from the others. In figure ??, we observe that a significant proportion of samples are memorized. For example, 10% of samples get a LiRA score of more~~

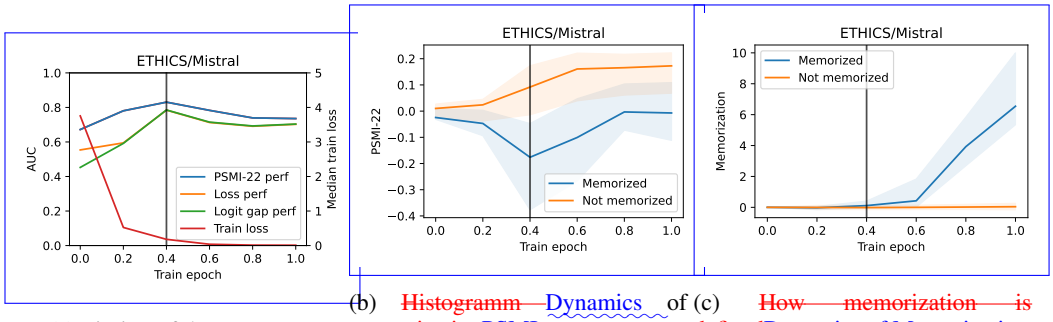

(a) Timing of the measure (b) ~~Histogramm~~ Dynamics of ~~memorization~~PSMI (c) ~~How memorization is defined~~Dynamics of Memorization

Figure 3: ~~Subfigure~~ Memorized samples can be detected from epoch 0.4, though they are not yet memorized. Figure 3a: in blue, orange and green, the ~~FPR@TPR=0.75~~ AUC of PSMI~~(layer 32)~~, Loss and Logit Gap ~~to predict memorization~~; in red, the median train loss. The vertical line ~~is~~ marks the ~~first checkpoint where the median train loss has decreased by~~ 95% ~~; it is the first where memorization can be predicted effectively~~decrease in training loss. ~~Subfigure ??~~Figure 3b: ~~histogram of log-LiRA scores at epoch 10. The 10% quantile corresponds to LiRA $\geq e^{3.16} \simeq 23.5$, which indicates strong memorization. Subfigure ??: impact of~~ the ~~quantile applied on LiRA at epoch 10 to define "memorized" and "not memorized" samples.Impact of the choice of the layer on the performance of PSMI to predict memorization. The~~ solid ~~lines represent~~ line shows the ~~FPR@TPR=0.75 for the~~ median PSMI ~~predictor at that layer,~~ for memorized and ~~the dashed lines represent the performance of the Loss predictor~~non-memorized samples, ~~which does not depend of~~ while the ~~layer. **Left:** in every setting, only~~ shaded area represents the ~~last layers are effective to predict memorization~~25%-75% quantiles. ~~**Middle:** zoom on the most important layers for~~ Figure 3c outlines memorization using a ~~fixed model (Mistral)~~similar representation.~~**Right:** zoom on the most important layers for a fixed dataset (MMLU). The shape of the profile depends more of the dataset than the model. For easier tasks like binary classification (ETHICS), the most relevant layers are the last ones, while for other datasets, layers of intermediate depth are also significant.~~

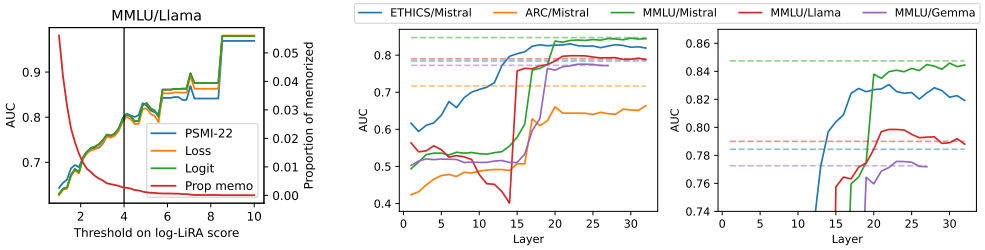

(a) How memorization is defined (b) Impact of the choice of layer

Figure 4: Figure 4a: impact of the threshold used to define "memorized" and "non-memorized" samples. The vertical bar indicates the default threshold log-LiRA = 4. Figure 4b: impact of the choice of the layer on the performance of PSMI. The solid lines represent the AUC for PSMI at that layer, and the dashed lines represent the AUC for the loss, which does not depend on the layer. The right plot is a zoomed-in view focusing on high AUC regions.

than $e^{3.16} \simeq 23.5$As said at the beginning of Section 3, memorized samples are defined by default as the one with log-LiRA ≥ 4, which means LiRA $\geq e^4 \simeq 54.6$. This indicates strong memorizationbecause , as the attack predicts that these elements are 23.5 54.6 more likely to be members of the dataset than non-member (see details in appendix Appendix A.1.1). By default, we used the 10% quantile to define memorization for all experiments we present in this paper.

In figure ?? we see that our approach remains efficient for a broad range of thresholds used to define memorization, with a FPR@TPR=0.75 below 13% even when we define that 25% of samples are memorized . This corresponds to a very low LiRA threshold(equal to $e^{1.20} \simeq 3.3$). Unsurprisingly, both PSMI and the loss are more efficient at targetting elements with very high LiRA score, corresponding to low quantiles in figure ??. This is because For example, with MMLU/Llama, 2.8% of the elements meet this definition after one epoch of training (see Appendix D.2 for results in other settings). In Figure 4a, we vary this threshold and measure the AUC using PSMI, loss and logit gap. We also represent the proportion of memorized samples associated with the threshold. We observe that our method is more effective for most vulnerable samples, getting the highest log-LiRA score. We interpret this as meaning that elements that are obviously detected as memorized by LiRA were necessarily hard to learn for the model, so they can be detected by our method. There are other methods to measure memorization in a language model, such as counterfactual memorization. See appendix A.2 for a comparison between these definitionsSee Appendix A.2 and Appendix D.3 for additional results and discussions.

Impact of the layer used to compute PSMI (Figure 4b) The default method presented in algorithm 1 uses hidden representations at the last layer to predict memorization. However, depending on the model and the dataset, different layers can be more effective, as we can see in figure 4b. We observe that in every setting, only the last layers are useful to predict memorization. However, it appears that layers have different importance depending on the dataset. When we fix the model to Mistral and vary the dataset, we observe that for complex tasks such as MMLU or ARC datasets (with up to 5 possible labels), all layers starting from the 20th are relevant to predict memorization, with minor variation after the 20th layerthe curve rises sharply around layers 15–20 and then stabilizes with minor variations. We interpret this to mean that more complex tasks require more intricate interactions between tokens representation, so relevant layers are concentrated at the end of the network. On the opposite, for ETHICS dataset, which is a simpler task of binary classification, effective layers are concentrated at the end of the model (after the 29th layer). We interpret this to mean that more complex tasks require more intricate interactions between token representations, so a greater number of layersare crucial during fine-tuningthe curve increases more smoothly. This indicates that samples are easier to separate with fewer interactions between tokens, allowing memorization to be detected from the earliest layers. Conversely, we observed that for a fixed dataset (MMLU), the choice of the model has little impact on the shape of the curve. Finally, we observe that across all settings, the difference between the AUC with the last layer and the AUC with the best layer is minor, which justifies selecting the last layer in Algorithm 1.

Applicability to other classification settings (Figure 5) As noted in Section 1.2, our method relies on the specific properties of neither LLMs nor fine-tuning. Consequently, it is suitable for any model trained for classification tasks. To validate this hypothesis, we applied our method as-is to a Wide Residual Network WRN16-4 (Zagoruyko & Komodakis, 2016) trained from scratch on CIFAR-10. This setting differs significantly from the fine-tuning of LLMs studied so far: the model uses convolutions instead of transformers, is trained on a visual task rather than a textual one, and is trained from scratch rather than fine-tuned. We believe that the excellent performance of our method in this setting indicates that it is applicable to a wide range of classification scenarios.

We adapted the framework of Aerni et al. (2024) to interrupt training and measure the PSMI, loss, and logit gap on a model trained without any mitigation techniques. The authors have introduced out-of-distribution *canaries* within the training set, and have demonstrated that they correctly mimic the most vulnerable samples. In Figure 5a, we predict memorization using the same definition as above, with a threshold of 4 applied to log-LiRA. Even though our method was applied without any modifications, we obtain very high AUC scores, surpassing those achieved with MMLU/Mistral, which is our best setting for fine-tuned LLMs. However, we note that the defaults hyperparameters of Algorithm 1 leads to a very good FPR, but a low TPR. Indeed, in this setting, 3.8% of samples satisfy log-LiRA ≥ 4, which is relatively high (see Appendix D.2). In contrast, in Figure 5b, we

focus on the most vulnerable samples by predicting the canaries that mimic them. We observe that our method yields excellent results, and that the hyperparameters of Algorithm 1 are well-suited for detecting these highly vulnerable samples. In Figure 5c, we confirm that our method obtains better results when detecting samples that are very well memorized, with a high log-LiRA score (see Appendix D.5 for more details).

4 Final remarks

Ethical considerations This paper discusses vulnerability to privacy attacks against language models in practical settings. This raises ethical considerations because similar models trained on private data have already been attacked in production (Nasr et al., 2023). However, we believe that our work is unlikely to benefit adversaries with harmful intent, for several reasons. First, our approach necessitates access to the checkpoint of a partially trained model, and to the training dataset. In practice, adversaries do not possess this capability, making it impossible for them to apply our method. Second, even though our work improves our understanding of unintended memorization, we believe that this will benefit privacy researchers more than adversaries. Indeed, it can help practitioners to better audit models under development, and empirical defenses could be derived from our work in the future.

Limitations and future works ~~We only evaluated our work on language models~~ Our method is specifically applicable to classification tasks. Most of our experiments focus on LLMs fine-tuned ~~on textual classificationapplied to multi-choice question~~for textual classification, applied to multiple-choice questions. We used this setting because some datasets such as MMLU are known to be challenging for language models and are often used to evaluate models' abilities. However, it would be interesting to ~~assess our method in other settings. The theorem we demonstrated and the algorithm we proposed are readily adaptable to any transformer-based model trained on any classification task. For example, our approach could be evaluated on vision models or multimodal models. Moreover, it would be interesting to modify our algorithm to evaluate it on self-supervised learning taskssuch as next-token-prediction. This task is indeed widely used, and it~~ explore whether our method can be modified to be applicable to LLMs trained on generative tasks. This is indeed a widely used scenario, which is known to ~~be prone to memorization~~entail very high privacy risks.

Moreover, the approach we developed to predict memorization from the early stages of training could be used to develop empirical defenses. Indeed, numerous methods have been developed to defend against unintended memorization in practice, with good privacy-utility trade-offs (Chen et al., 2022; Tang et al., 2022; Chen & Pattabiraman, 2024; Aerni et al., 2024). Our algorithm could be employed to design adaptive defenses that concentrate their efforts on most vulnerable samples to improve the privacy-utility trade-off.

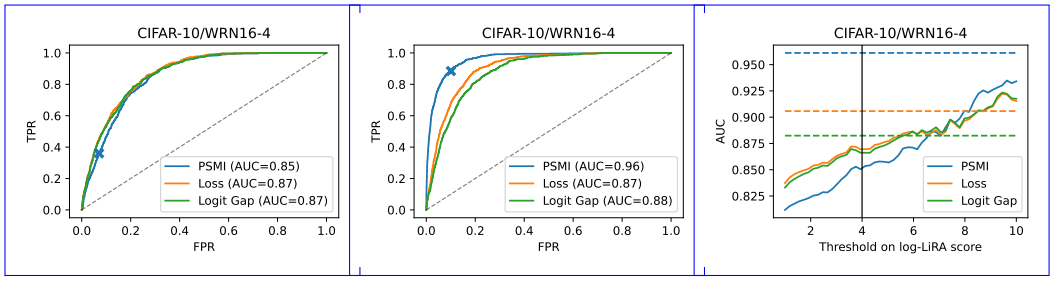

(a) Detecting memorization (b) Detecting canaries (c) How memorization is defined

Figure 5: Applying our method as-is on a WRN16-4 trained from scratch on CIFAR-10, adapting the framework of Aerni et al. (2024). Figure 5a: Using PSMI (last layer), loss and logit gap to predict memorized samples. The cross marks the default hyperparameters of Algorithm 1. Figure 5b: Predicting canaries that mimic most memorized samples. Figure 5c The solid line represents the impact of the choice of threshold applied to LiRA to defined "memorized" and "non memorized" samples. The dashed line is the AUC when memorized samples are defined as the canaries.

Reproducibility statement We have detailed all essential hyperparameters necessary to reproduce our experiments. In addition, we provide the following repository containing the Python, Bash and Slurm scripts that we used to deploy our experiments on an HPC cluster. We also provide a PyPI package containing an automated estimator of PSMI that can be used in a wide range of scenarios.

hidden_github_url_experiment_repo_for_review
hidden_github_url_pypi_package_for_review

~~To ensure the reproducibility of our experimental results, we repeated our experiments using different random seeds for the same datasets and architecture. We obtained similar results, which confirms the reliability of our empirical findings (see appendix **??**).~~

5 Conclusion

In this work, we demonstrate that it is possible to predict which samples will be memorized by a language model in a classification setting. Our metric ~~, based on Pointwise Sliced Mutual Information,~~ is computationally efficient, and it can be utilized from the early stages of training. We provide a theoretical justification for our approach, and we validate its effectiveness on three different language model architectures fine-tuned on three different classification datasets. Moreover, we ~~provide default hyperparameters to make our method easily applicable by practitioners willing to audit models under realistic conditions~~demonstrate that our method is easily applicable to other classification scenarios by successfully applying it, without modification, to a vision model trained from scratch. We view this method as a first step towards developing useful tools to evaluate models during training, understand the privacy risks they entail, and prevent unintended memorization in the most efficient way.

Hidden acknowledgements for double-blind reviews.

References

Michael Aerni, Jie Zhang, and Florian Tramèr. Evaluations of Machine Learning Privacy Defenses are Misleading. In *ACM CCS*, April 2024. URL http://arxiv.org/abs/2404.17399.

Devansh Arpit, Stanisław Jastrzebski, Nicolas Ballas, David Krueger, Emmanuel Bengio, Maxinder S. Kanwal, Tegan Maharaj, Asja Fischer, Aaron Courville, Yoshua Bengio, and Simon Lacoste-Julien. A Closer Look at Memorization in Deep Networks. In *ICML*, volume 70, pp. 233–242, August 2017. URL https://proceedings.mlr.press/v70/arpit17a.html.

Achraf Azize and Debabrota Basu. How Much Does Each Datapoint Leak Your Privacy? Quantifying the Per-datum Membership Leakage. In *Theory and Practice of Differential Privacy*, February 2024. URL http://arxiv.org/abs/2402.10065.

Stella Biderman, Usvsn Sai Prashanth, Lintang Sutawika, Hailey Schoelkopf, Quentin Anthony, Shivanshu Purohit, and Edward Raff. Emergent and Predictable Memorization in Large Language Models. In *NeurIPS*, volume 36, pp. 28072–28090, 2023. URL https://proceedings.neurips.cc/paper_files/paper/2023/file/59404fb89d6194641c69ae99ecdf8f6d-Paper-Conference.pdf.

Michael Boratko, Harshit Padigela, Divyendra Mikkilineni, Pritish Yuvraj, Rajarshi Das, Andrew McCallum, Maria Chang, Achille Fokoue-Nkoutche, Pavan Kapanipathi, Nicholas Mattei, Ryan Musa, Kartik Talamadupula, and Michael Witbrock. A Systematic Classification of Knowledge, Reasoning, and Context within the ARC Dataset. In *Proceedings of the Workshop on Machine Reading for Question Answering*, pp. 60–70, 2018. doi: 10.18653/v1/W18-2607. URL http://aclweb.org/anthology/W18-2607.

Nicholas Carlini, Chang Liu, Úlfar Erlingsson, Jernej Kos, and Dawn Song. The Secret Sharer: Evaluating and Testing Unintended Memorization in Neural Networks. In *USENIX Security*, pp. 267–284, 2018. URL https://www.usenix.org/conference/usenixsecurity19/presentation/carlini.

Nicholas Carlini, Florian Tramer, Eric Wallace, Matthew Jagielski, Ariel Herbert-Voss, Katherine Lee, Adam Roberts, Tom B Brown, Dawn Song, Ulfar Erlingsson, Alina Oprea, and Colin Raffel. Extracting Training Data from Large Language Models. In *USENIX Security*, 2021. URL https://www.usenix.org/conference/usenixsecurity21/presentation/carlini-extracting.

Nicholas Carlini, Steve Chien, Milad Nasr, Shuang Song, Andreas Terzis, and Florian Tramèr. Membership Inference Attacks From First Principles. In *IEEE S&P*, pp. 1897–1914, 2022a. doi: 10.1109/SP46214.2022.9833649. URL https://ieeexplore.ieee.org/document/9833649/.

Nicholas Carlini, Matthew Jagielski, Chiyuan Zhang, Nicolas Papernot, Andreas Terzis, and Florian Tramer. The Privacy Onion Effect: Memorization is Relative. In *NeurIPS*, 2022b. URL https://proceedings.neurips.cc/paper_files/paper/2022/file/564b5f8289ba846ebc498417e834c253-Paper-Conference.pdf.

Nicholas Carlini, Daphne Ippolito, Matthew Jagielski, Katherine Lee, Florian Tramer, and Chiyuan Zhang. Quantifying Memorization Across Neural Language Models. In *ICLR*, 2023. URL https://openreview.net/forum?id=TatRHT_1cK.

Satrajit Chatterjee. Learning and Memorization. In *ICML*, volume 80, pp. 755–763, 2018. URL https://proceedings.mlr.press/v80/chatterjee18a.html.

Dingfan Chen, Ning Yu, and Mario Fritz. RelaxLoss: Defending Membership Inference Attacks without Losing Utility. In *ICLR*, 2022. URL https://openreview.net/forum?id=FEDfGWVZYIn.

Zitao Chen and Karthik Pattabiraman. Overconfidence is a Dangerous Thing: Mitigating Membership Inference Attacks by Enforcing Less Confident Prediction. In *NDSS*, 2024. URL https://www.ndss-symposium.org/wp-content/uploads/2024-14-paper.pdf.

Zeyu Cui, Jianxin Ma, Chang Zhou, Jingren Zhou, and Hongxia Yang. M6-Rec: Generative Pretrained Language Models are Open-Ended Recommender Systems, May 2022. URL http://arxiv.org/abs/2205.08084. arXiv:2205.08084 [cs].

Jérémie Dentan, Arnaud Paran, and Aymen Shabou. Reconstructing training data from document understanding models. In *USENIX Security*, pp. 6813–6830, 2024. URL https://www.usenix.org/conference/usenixsecurity24/presentation/dentan.

Mohamed Dhouib, Ghassen Bettaieb, and Aymen Shabou. DocParser: End-to-end OCR-free Information Extraction from Visually Rich Documents. In *ICDAR*, May 2023. URL https://arxiv.org/abs/2304.12484.

Vitaly Feldman. Does learning require memorization? a short tale about a long tail. In *ACM SIGACT STOC*, pp. 954–959, June 2020. doi: 10.1145/3357713.3384290. URL https://dl.acm.org/doi/10.1145/3357713.3384290.

Vitaly Feldman and Chiyuan Zhang. What Neural Networks Memorize and Why: Discovering the Long Tail via Influence Estimation. In *NeurIPS*, 2020. URL https://proceedings.neurips.cc/paper/2020/hash/1e14bfe2714193e7af5abc64ecbd6b46-Abstract.html.

Shijie Geng, Shuchang Liu, Zuohui Fu, Yingqiang Ge, and Yongfeng Zhang. Recommendation as Language Processing (RLP): A Unified Pretrain, Personalized Prompt & Predict Paradigm (P5). In *Proceedings of the 16th ACM Conference on Recommender Systems*, pp. 299–315, September 2022. ISBN 978-1-4503-9278-5. doi: 10.1145/3523227.3546767. URL https://dl.acm.org/doi/10.1145/3523227.3546767.

Ziv Goldfeld and Kristjan Greenewald. Sliced Mutual Information: A Scalable Measure of Statistical Dependence. In *NeurIPS*, volume 34, pp. 17567–17578, 2021. URL https://proceedings.neurips.cc/paper_files/paper/2021/file/92c4661685bf6681f6a33b78ef729658-Paper.pdf.

Peter Henderson, Xuechen Li, Dan Jurafsky, Tatsunori Hashimoto, Mark A. Lemley, and Percy Liang. Foundation Models and Fair Use. *JMLR*, pp. 1–79, 2024. URL http://jmlr.org/papers/v24/23-0569.html.

Dan Hendrycks, Collin Burns, Steven Basart, Andrew Critch, Jerry Li, Dawn Song, and Jacob Steinhardt. Aligning AI With Shared Human Values. In *ICLR*, 2021a. URL https://openreview.net/forum?id=dNy_RKzJacY.

Dan Hendrycks, Collin Burns, Steven Basart, Andy Zou, Mantas Mazeika, Dawn Song, and Jacob Steinhardt. Measuring Massive Multitask Language Understanding. In *ICLR*, 2021b. URL https://openreview.net/forum?id=d7KBjmI3GmQ.

Marius Hobbhahn and Jsevillamol. What's the backward-forward FLOP ratio for Neural Networks? *lesswrong*, December 2021. URL https://www.lesswrong.com/posts/fnjKpBoWJXcSDwhZk/what-s-the-backward-forward-flop-ratio-for-neural-networks.

Edward J. Hu, Yelong Shen, Phillip Wallis, Zeyuan Allen-Zhu, Yuanzhi Li, Shean Wang, Lu Wang, and Weizhu Chen. LoRA: Low-Rank Adaptation of Large Language Models. In *ICLR*, 2022. URL https://openreview.net/forum?id=nZeVKeeFYf9.

Albert Q. Jiang, Alexandre Sablayrolles, Arthur Mensch, Chris Bamford, Devendra Singh Chaplot, Diego de las Casas, Florian Bressand, Gianna Lengyel, Guillaume Lample, Lucile Saulnier, Lélio Renard Lavaud, Marie-Anne Lachaux, Pierre Stock, Teven Le Scao, Thibaut Lavril, Thomas Wang, Timothée Lacroix, and William El Sayed. Mistral 7B, October 2023. URL http://arxiv.org/abs/2310.06825.

Geewook Kim, Teakgyu Hong, Moonbin Yim, JeongYeon Nam, Jinyoung Park, Jinyeong Yim, Wonseok Hwang, Sangdoo Yun, Dongyoon Han, and Seunghyun Park. OCR-Free Document Understanding Transformer. In *ECCV*, 2022. URL https://arxiv.org/abs/2111.15664.

Jooyoung Lee, Thai Le, Jinghui Chen, and Dongwon Lee. Do Language Models Plagiarize? In *ACM WWW*, pp. 3637–3647, 2023. doi: 10.1145/3543507.3583199. URL https://dl.acm.org/doi/abs/10.1145/3543507.3583199.

Katherine Lee, Daphne Ippolito, Andrew Nystrom, Chiyuan Zhang, Douglas Eck, Chris Callison-Burch, and Nicholas Carlini. Deduplicating Training Data Makes Language Models Better. In *ALC*, pp. 8424–8445, 2022. doi: 10.18653/v1/2022.acl-long.577. URL https://aclanthology.org/2022.acl-long.577.

Tobias Leemann, Bardh Prenkaj, and Gjergji Kasneci. Is My Data Safe? Predicting Instance-Level Membership Inference Success for White-box and Black-box Attacks. In *ICML 2024 Next Generation of AI Safety Workshop*, 2024. URL https://openreview.net/forum?id=YfzvhsKymO.

Pietro Lesci, Clara Meister, Thomas Hofmann, Andreas Vlachos, and Tiago Pimentel. Causal Estimation of Memorisation Profiles. In *ACL*, 2024. URL https://aclanthology.org/2024.acl-long.834/.

Nils Lukas, Ahmed Salem, Robert Sim, Shruti Tople, Lukas Wutschitz, and Santiago Zanella-Béguelin. Analyzing Leakage of Personally Identifiable Information in Language Models. In *IEEE S&P*, May 2023. doi: 10.1109/SP46215.2023.10179300. URL https://www.computer.org/csdl/proceedings-article/sp/2023/933600a346/1OXH3fH5lIs.

Prasanta Chandra Mahalanobis. On the Generalized Distance in Statistics. In *Proceedings of the National Institute of Science of India*, volume 12, pp. 49–55. National Institute of Science of India, 1936.

Justus Mattern, Fatemehsadat Mireshghallah, Zhijing Jin, Bernhard Schoelkopf, Mrinmaya Sachan, and Taylor Berg-Kirkpatrick. Membership Inference Attacks against Language Models via Neighbourhood Comparison. In *Findings of the ACL*, pp. 11330–11343, 2023. doi: 10.18653/v1/2023.findings-acl.719. URL https://aclanthology.org/2023.findings-acl.719.

Alexander G. de G. Matthews, Jiri Hron, Mark Rowland, Richard E. Turner, and Zoubin Ghahramani. Gaussian Process Behaviour in Wide Deep Neural Networks. In *ICLR*, 2018. URL https://openreview.net/forum?id=H1-nGgWC-.

Matthieu Meeus, Igor Shilov, Manuel Faysse, and Yves-Alexandre de Montjoye. Copyright Traps for Large Language Models. In *ICML*, 2024. URL https://openreview.net/forum?id=LDq1JPdc55.

Sewon Min, Suchin Gururangan, Eric Wallace, Hannaneh Hajishirzi, Noah A. Smith, and Luke Zettlemoyer. SILO Language Models: Isolating Legal Risk In a Nonparametric Datastore, August 2023. URL http://arxiv.org/abs/2308.04430. arXiv:2308.04430 [cs].

Fatemehsadat Mireshghallah, Kartik Goyal, Archit Uniyal, Taylor Berg-Kirkpatrick, and Reza Shokri. Quantifying Privacy Risks of Masked Language Models Using Membership Inference Attacks. In *ACL-EMNLP*, November 2022a. doi: 10.18653/v1/2022.emnlp-main.570.

Fatemehsadat Mireshghallah, Archit Uniyal, Tianhao Wang, David Evans, and Taylor Berg-Kirkpatrick. An Empirical Analysis of Memorization in Fine-tuned Autoregressive Language Models. In *ACL-EMNLP*, pp. 1816–1826, December 2022b. doi: 10.18653/v1/2022.emnlp-main.119. URL https://aclanthology.org/2022.emnlp-main.119/.

Milad Nasr, Nicholas Carlini, Jonathan Hayase, Matthew Jagielski, A. Feder Cooper, Daphne Ippolito, Christopher A. Choquette-Choo, Eric Wallace, Florian Tramèr, and Katherine Lee. Scalable Extraction of Training Data from (Production) Language Models, November 2023. URL http://arxiv.org/abs/2311.17035.

Aneesh Pappu, Billy Porter, Ilia Shumailov, and Jamie Hayes. Measuring memorization in RLHF for code completion, October 2024. URL http://arxiv.org/abs/2406.11715. arXiv:2406.11715 [cs].

USVSN Sai Prashanth, Alvin Deng, Kyle O'Brien, Jyothir S V, Mohammad Aflah Khan, Jaydeep Borkar, Christopher A. Choquette-Choo, Jacob Ray Fuehne, Stella Biderman, Tracy Ke, Katherine Lee, and Naomi Saphra. Recite, Reconstruct, Recollect: Memorization in LMs as a Multifaceted Phenomenon, June 2024. URL http://arxiv.org/abs/2406.17746. arXiv:2406.17746 [cs].

Reza Shokri, Marco Stronati, Congzheng Song, and Vitaly Shmatikov. Membership Inference Attacks against Machine Learning Models. In *IEEE S&P*, 2017. doi: 10.1109/SP.2017.41. URL https://www.computer.org/csdl/proceedings-article/sp/2017/07958568/12OmNBUAvVc.

Xinyu Tang, Saeed Mahloujifar, Liwei Song, Virat Shejwalkar, Milad Nasr, Amir Houmansadr, and Prateek Mittal. Mitigating Membership Inference Attacks by Self-Distillation Through a Novel Ensemble Architecture. In *USENIX Security*, pp. 1433–1450, 2022. URL https://www.usenix.org/conference/usenixsecurity22/presentation/tang.

Gemma Team, Thomas Mesnard, Cassidy Hardin, Robert Dadashi, Surya Bhupatiraju, Shreya Pathak, Laurent Sifre, Morgane Rivière, Mihir Sanjay Kale, Juliette Love, Pouya Tafti, Léonard Hussenot, Pier Giuseppe Sessa, Aakanksha Chowdhery, Adam Roberts, Aditya Barua, Alex Botev, Alex Castro-Ros, Ambrose Slone, Amélie Héliou, Andrea Tacchetti, Anna Bulanova, Antonia Paterson, Beth Tsai, Bobak Shahriari, Charline Le Lan, Christopher A. Choquette-Choo, Clément Crepy, Daniel Cer, Daphne Ippolito, David Reid, Elena Buchatskaya, Eric Ni, Eric Noland, Geng Yan, George Tucker, George-Christian Muraru, Grigory Rozhdestvenskiy, Henryk Michalewski, Ian Tenney, Ivan Grishchenko, Jacob Austin, James Keeling, Jane Labanowski, Jean-Baptiste Lespiau, Jeff Stanway, Jenny Brennan, Jeremy Chen, Johan Ferret, Justin Chiu, Justin Mao-Jones, Katherine Lee, Kathy Yu, Katie Millican, Lars Lowe Sjoesund, Lisa Lee, Lucas Dixon, Machel Reid, Maciej Mikuła, Mateo Wirth, Michael Sharman, Nikolai Chinaev,

Nithum Thain, Olivier Bachem, Oscar Chang, Oscar Wahltinez, Paige Bailey, Paul Michel, Petko Yotov, Rahma Chaabouni, Ramona Comanescu, Reena Jana, Rohan Anil, Ross McIlroy, Ruibo Liu, Ryan Mullins, Samuel L. Smith, Sebastian Borgeaud, Sertan Girgin, Sholto Douglas, Shree Pandya, Siamak Shakeri, Soham De, Ted Klimenko, Tom Hennigan, Vlad Feinberg, Wojciech Stokowiec, Yu-hui Chen, Zafarali Ahmed, Zhitao Gong, Tris Warkentin, Ludovic Peran, Minh Giang, Clément Farabet, Oriol Vinyals, Jeff Dean, Koray Kavukcuoglu, Demis Hassabis, Zoubin Ghahramani, Douglas Eck, Joelle Barral, Fernando Pereira, Eli Collins, Armand Joulin, Noah Fiedel, Evan Senter, Alek Andreev, and Kathleen Kenealy. Gemma: Open Models Based on Gemini Research and Technology, April 2024. URL http://arxiv.org/abs/2403.08295.

Hugo Touvron, Thibaut Lavril, Gautier Izacard, Xavier Martinet, Marie-Anne Lachaux, Timothée Lacroix, Baptiste Rozière, Naman Goyal, Eric Hambro, Faisal Azhar, Aurelien Rodriguez, Armand Joulin, Edouard Grave, and Guillaume Lample. LLaMA: Open and Efficient Foundation Language Models, February 2023. URL https://arxiv.org/abs/2302.13971.

Wenhao Wang, Muhammad Ahmad Kaleem, Adam Dziedzic, Michael Backes, Nicolas Papernot, and Franziska Boenisch. Memorization in Self-Supervised Learning Improves Downstream Generalization. In *ICLR*, 2024. URL https://openreview.net/forum?id=KSjPaXtxP8.

Yuxin Wen, Arpit Bansal, Hamid Kazemi, Eitan Borgnia, Micah Goldblum, Jonas Geiping, and Tom Goldstein. Canary in a Coalmine: Better Membership Inference with Ensembled Adversarial Queries. In *ICLR*, 2023. URL https://openreview.net/forum?id=b7SBTEBFnC.

Shelvia Wongso, Rohan Ghosh, and Mehul Motani. Pointwise Sliced Mutual Information for Neural Network Explainability. In *IEEE ISIT*, pp. 1776–1781, June 2023a. doi: 10.1109/ISIT54713.2023.10207010. URL https://ieeexplore.ieee.org/document/10207010/.

Shelvia Wongso, Rohan Ghosh, and Mehul Motani. Using Sliced Mutual Information to Study Memorization and Generalization in Deep Neural Networks. In *ICAIS*, volume 206, pp. 11608–11629, April 2023b. URL https://proceedings.mlr.press/v206/wongso23a.html.

Samuel Yeom, Irene Giacomelli, Matt Fredrikson, and Somesh Jha. Privacy Risk in Machine Learning: Analyzing the Connection to Overfitting. In *IEEE CSF*, pp. 268–282, 2018. doi: 10.1109/CSF.2018.00027. URL https://www.computer.org/csdl/proceedings-article/csf/2018/668001a268/12OmNyQGSca.

Weichen Yu, Tianyu Pang, Qian Liu, Chao Du, Bingyi Kang, Yan Huang, Min Lin, and Shuicheng Yan. Bag of Tricks for Training Data Extraction from Language Models. In *ICML*, June 2023. URL https://dl.acm.org/doi/abs/10.5555/3618408.3620094.

Sergey Zagoruyko and Nikos Komodakis. Wide Residual Networks. In *BMVC*, pp. 87.1–87.12, 2016. doi: 10.5244/C.30.87. URL http://www.bmva.org/bmvc/2016/papers/paper087/index.html.

Sajjad Zarifzadeh, Philippe Liu, and Reza Shokri. Low-Cost High-Power Membership Inference Attacks, June 2024. URL http://arxiv.org/abs/2312.03262.

Chiyuan Zhang, Samy Bengio, Moritz Hardt, Benjamin Recht, and Oriol Vinyals. Understanding deep learning requires rethinking generalization. In *ICLR*, 2017. URL https://openreview.net/forum?id=Sy8gdB9xx.

Chiyuan Zhang, Daphne Ippolito, Katherine Lee, Matthew Jagielski, Florian Tramèr, and Nicholas Carlini. Counterfactual Memorization in Neural Language Models. In *NeurIPS*, 2023. URL https://neurips.cc/virtual/2023/poster/72772.

Xiangxin Zhu, Dragomir Anguelov, and Deva Ramanan. Capturing Long-Tail Distributions of Object Subcategories. In *IEEE CVPR*, pp. 915–922, June 2014. doi: 10.1109/CVPR.2014.122. URL https://ieeexplore.ieee.org/document/6909517.

Jakub Šmíd, Pavel Priban, and Pavel Kral. LLaMA-Based Models for Aspect-Based Sentiment Analysis. In *Proceedings of the 14th Workshop on Computational Approaches to Subjectivity, Sentiment, & Social Media Analysis*, pp. 63–70, 2024. doi: 10.18653/v1/2024.wassa-1.6. URL https://aclanthology.org/2024.wassa-1.6.

A DEFINING AND MEASURING MEMORIZATION FOR CLASSIFICATION TASKS

Defining and measuring memorization for classification tasks is a challenging task. ~~In section~~ As explained in Section 1.1, vulnerability to extraction attacks is rarely used for such models. Conversely, in these settings, it is standard to define memorization as vulnerability to membership inference attacks such as LiRA or to use counterfactual memorization. In Section A.1, we present two variants of LiRA ~~membership inference attack~~ (Carlini et al., 2022a): a local version (used in the main body of the paper), which targets a fixed model and its training set, and a global version, which targets a dataset used to train multiple models. In ~~section~~ Section A.2, we compare LiRA and counterfactual memorization. It appears that these two definitions are consistent with each others, especially for highly memorized samples. This confirms the relevance of choosing LiRA as the ground truth memorization for our experiments. ~~Finally, in section D.1, we discuss the impact of when to stop training to measure ground truth memorization.~~

A.1 LIRA ATTACK

A.1.1 ATTACKING A MODEL: LOCAL VERSION

In this section we present the original version of LiRA (Carlini et al., 2022a). We call it the *local* version, because it targets a fixed model and tries to determine if a target sample was part of its training set. Note that this setting is aligned with our threat model (~~see section~~ See Section 1.2): the model is fixed; and for each sample, if the attack confidently predict that it was part of the training set, we say that it is memorized. This is why we used this *local* version in the main body of this paper.

Notations Let $\mathbf{X} = \{(x_i, y_i)\}_{i \in [\![1,N]\!]}$ be a training set of N labelled elements. We focus on multi-choice question (MCQ) academic benchmarks such as MMLU (Hendrycks et al., 2021b). Let S be a random variable representing a subset of elements in $[\![1, N]\!]$. Let $\mathbf{X}_S = \{(x_i, y_i) \mid i \in S\}$ be the corresponding subset of training elements, and $f_S \sim \mathcal{T}(X_S)$ be a model trained on this subset with the randomized training procedure $\mathcal{T}$. Then, let $\mathcal{L}(x, f_S)$ be the logit gap of the evaluation of x with model f_S, i.e. the difference between the highest and second-highest logit.

The Likelihood Ratio Attack (LiRA) Let fix a target subset S^*, a target model $f_{S^*} \sim \mathcal{T}(\mathbf{X}_{S^*})$ trained on these elements, and a target element $x \in \mathbf{X}$. As every membership inference attack, LiRA aims to determine whether x was in $\mathbf{X}_{S^*}$. First, we train a great number of *shadow models* f_S on random subsets of $\mathbf{X}$, and evaluates the logit gap $\mathcal{L}(x, f_S)$ for theses shadow ~~model~~models. Then, we gather $\mathcal{L}^{\text{in}} = \{\mathcal{L}(x, f_S) \mid x \in S\}$, the logit gaps of model that were trained on x ; and $\mathcal{L}^{\text{out}}$ for models that were not trained on x. We model these two sets as Gaussian distributions, and compute the probabilities p^{in} and p^{out} of the target logit gap $\mathcal{L}(x, f_{S^*})$ under these distributions.

The original LiRA score of Carlini et al. (2022a) is defined as $\text{LiRA}(x, f_S^*) = p^{\text{in}}/p^{\text{out}}$. However, it takes very high and low values positive values. For convenient representations in our graphs, we used the natural logarithm of this score in the main body of this paper. A value greater that 0 indicates that the sample is memorized, because $p^{\text{in}} > p^{\text{out}}$. For example, a value of 4 ~~already~~ indicates strong memorization, because it means that ~~$p^{\text{in}} \geq e^4 \cdot p^{\text{out}} \simeq 54.5 \cdot p^{\text{out}}$~~ $p^{\text{in}} \geq e^4 \cdot p^{\text{out}} \simeq 54.6 \cdot p^{\text{out}}$. In other words, the attack suggests that it is ~~54.5~~ 54.6 times more likely that the target samples belongs to the dataset of the target model, which is significant. This is why, unless otherwise stated, memorized samples are defined as the ones with log-LiRA ≥ 4 for our experiments in Section 3.

The number of shadow model needed to compute LiRA score is an important hyperparameter. In our experiments, we used 100 shadow models to evaluate memorization in each setting, which is in line with the empirical findings of Carlini et al. (2022a).

A.1.2 ATTACKING A DATASET: GLOBAL VERSION

It is also possible to use another version of LiRA, as in (Carlini et al., 2022b) for example. We call it the *global* version, because it does not target a fixed model; on the opposite, it attacks multiple models trained on a random splits of the same datasets, and measures the attack success rate of LiRA against each samples, which is defined below.

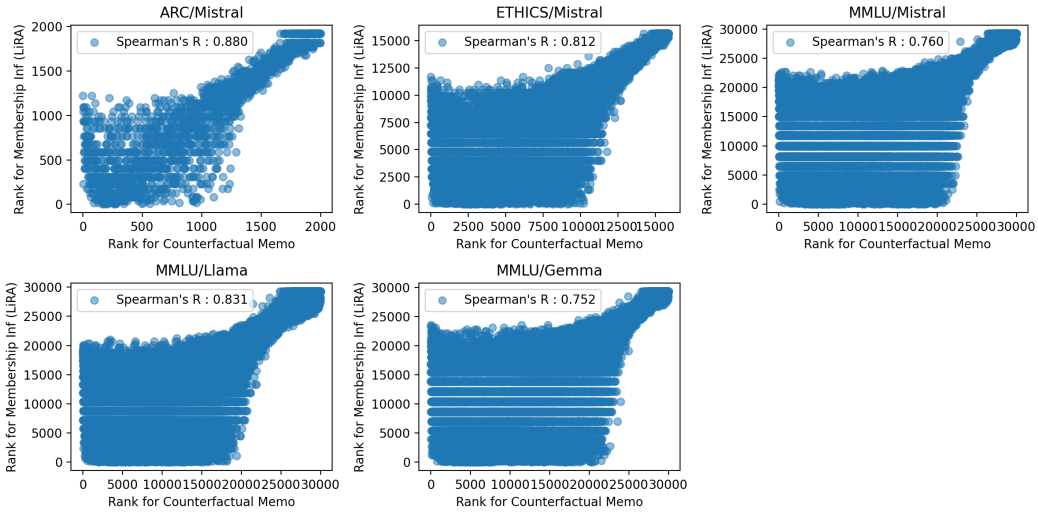

Figure 6: Comparing two definitions of memorization: counterfactual memorization (Feldman & Zhang, 2020; Zhang et al., 2023) and LiRA membership inference (Carlini et al., 2022a). We measure Spearmans'R coefficient to evaluate the consistency between the definitions. These experiments are conducted on models trained for 10 epochs.

The Attack Success Rate (ASR) It indicates whether a given element $x \in \mathbf{X}$ is likely to be memorized by any model trained on a subset $\mathbf{X}_S$ with training procedure $\mathcal{T}$. Let $\mathcal{D}$ be the distribution of S corresponding the choosing a random subset of $\lfloor N/2 \rfloor$ elements in $[\![1, N]\!]$, meaning that every element is selected with probability 50%. For every target element x, the attack success rate is computed as follows:

$$\mathrm{ASR}(x) = \mathop{\mathbb{P}}_{S\sim\mathcal{D},\, f_S\sim\mathcal{T}(\mathbf{X}_S)} \left[\mathbb{1}[p^{\text{in}} > p^{\text{out}}] = \mathbb{1}[x \in \mathbf{X}_S]\right] \tag{7}$$

~~**Differences compared to the local version**~~ ~~First, as said above, the~~ The global LiRA attack represents the likelihood that a sample in a dataset gets memorized by any model trained with a given procedure. As a result, this score is not consistent with our threat model. Indeed, in our threat model we want to audit a *fixed* model, because this is what practitioners do. This is why we did not use the global version in the main body of this paper.

~~Second, it is easier to set a threshold for the global version than for the local one. Indeed, for the local version, it may seem arbitrary, to set a threshold to separate memorized and non-memorized samples. This is why we preferred to use quantiles for that purpose in the main body of this paper (see section 3.2 and figure **??**). On the opposite, the global version is defined as a success rate, so we can define a p-value to quantify the significance of classifying a given x as memorized. We take as null hypothesis the scenario where x leaves no traces in the model, so each individual attack has a 50% chance of success. For example, using 100 shadow models to compute the ASR, a p-value of 10^{-9} corresponds to ASR $\geq 79\%$. This indicates a very reliable detection of memorization, because the size of our datasets is orders of magnitude smaller than 10^9, so we expect very few samples to be falsely classified as memorized.~~

A.2 Comparing several definitions of memorization

We compare two definitions of memorization: counterfactual memorization (Feldman & Zhang, 2020; Zhang et al., 2023) and vulnerability to LiRA membership inference attack (Carlini et al., 2022a). Counterfactual memorization is a *global* measure of memorization. Indeed, it quantifies the impact of a given sample x being in the training set on a population of model trained on random splits of a dataset. Similar to the global variant of LiRA (see ~~section~~ Section A.1.2), it is not in line with our threat model, because practitioners want to audit a *fixed* model, and not a population

of model trained on random splits of a dataset. Note that because counterfactual memorization is a global definition, we compared it to the global version of LiRA. We recall that this is not the one used in the main body of this paper (see ~~section~~ Section A.1). We used ~~equation~~ Equation 2 in (Zhang et al., 2023) to define counterfactual memorization. We used the logit gap as the performance metric M in their equation.

Our results are presented in ~~figure~~ Figure 6. We use Spearman's R score to quantify the consistency between the two definitions. Indeed, we are interested in the *order* of samples with respect to the memorization metric. We observe that Spearman's R between the two definition is high in every settings: it is always greater than 0.75, and escalates to 0.88 for Mistral models trained on ARC dataset. This demonstrates that LiRA and counterfactual memorization are consistent with each other. In addition, we can separate the samples in two groups: a first, weakly memorized group, for which there is greater variability between the two definitions (bottom left of the graphs), and a strongly memorized group, for which the two definitions are much more consistent with each other (top right of the graphs). The second group is the most important one in our setting, because we are interested in predicting memorized samples (and not predicting non-memorized ones).

The coherence of these two definitions, especially for highly memorized samples, confirms the relevance of choosing LiRA as the ground truth memorization for our experiments.

A.3 ~~When to stop training ?~~

~~**Top:** Training loss, testing loss, and epoch of the best testing loss for each experimental setting. **Middle:** Training accuracy, testing accuracy, and epoch of the best testing accuracy for each experimental setting. **Bottom:** TPR@FPR=0.75 for predicting memorization depending on whether we measure ground-truth memorization at epoch 7 or at epoch 10. The prediction is computed at the first checkpoint where the median training los has decreased by 95% (at epoch 0.2 or 0.4 depending on the setting).~~

~~As said in section 3, we always train the models for 10 epochs and measure memorization at the end. This ensures a fair comparison between each setting. However, as we observe in figure 8, checkpoint 10 is not always the one with the best testing accuracy. We evaluate the impact of the choice of epoch 10 to terminate training and measure memorization. We observe that the FPR@TPR=0.75 only varies by a few percents between epoch 7 and epoch 10, with minor variations between the PSMI and the loss. In each setting, we computed PSMI both at the layer with the best FPR@TPR=0.75 at epoch 10 and the second best layer (for example, layers 29 and 30 for ARC/Mistral).~~

B Proof of Theorem 1 and Discussion

In this section we prove Theorem 1 and discuss it. We recall the theorem:

Theorem 1 *Let $(X, Y) \in \mathbb{R}^d \times \{0, 1\}$ be random variables. We assume that $p(Y = 0) = p(Y = 1) = 0.5$ and that X is a continuous random variable. We also assume that there exist $\mu_0, \mu_1 \in \mathbb{R}^d$ with $\mu_0 \neq \mu_1$, and $\Sigma_0, \Sigma_1 \in \mathbb{R}^{d \times d}$, and a Bernoulli variable $\Delta \sim \mathcal{B}(\varepsilon)$ with $\varepsilon \in]0, 1[$ such that:*

$$p(X \mid Y = 0, \Delta = 0) \sim \mathcal{N}(\mu_0, \Sigma_0) \quad \text{and} \quad p(X \mid Y = 1, \Delta = 0) \sim \mathcal{N}(\mu_1, \Sigma_1) \tag{3}$$

$$\forall x \in \mathbb{R}^d, \quad p(Y = 0 \mid \Delta = 1, X = x) = p(Y = 1 \mid \Delta = 1, X = x) = 0.5 \tag{4}$$

Given this, we then have:

$$\mathop{\mathbb{E}}_{X,Y} [\text{PSMI}(X, Y) \mid \Delta = 0] > 0 \tag{5}$$

$$\mathop{\mathbb{E}}_{X,Y} [\text{PSMI}(X, Y) \mid \Delta = 1] \approx 0 \tag{6}$$

Proof of ~~equation~~ Equation 6 Let $x, y \in \mathbb{R}^d \times \{0, 1\}$. We use the hypothesis we made in ~~equation~~ Equation 4:

$$p(X = x, Y = y \mid \Delta = 1) = \frac{p(X = x, Y = y, \Delta = 1)}{p(\Delta = 1)} p(Y = \frac{p(Y = y \mid X = x, \Delta = 1) p(X = x, \Delta = 1)}{p(\Delta = 1)} y \mid \Delta = \frac{p(Y = 1}{} \tag{8}$$

$$= 0.5 \times p(X = x, Y \mid \Delta = 1) \tag{9}$$

$$= p(Y = y \mid \Delta = 1) \times p(X = x \mid \Delta = 1) \tag{10}$$

$$\tag{11}$$

~~This enables the change of variable:~~

$$\begin{aligned}
\mathop{\mathbb{E}}_{X,Y}[\text{PSMI}(X, Y) \mid \Delta = 1] &= \int_{X,Y} \text{PSMI}(X, Y) \mathrm{d}p(X, Y \mid \Delta = 1) \\
&= \int_{X,Y} \text{PSMI}(X, 1 - Y) \mathrm{d}p(X, 1 - Y \mid \Delta = 1) \\
&= \int_{X,Y} \text{PSMI}(X, 1 - Y) \mathrm{d}p(X, Y \mid \Delta = 1) \\
&= \mathop{\mathbb{E}}_{X,Y}[\text{PSMI}(X, 1 - Y) \mid \Delta = 1].
\end{aligned}$$

~~Now, we can compute:~~

$$\begin{aligned}
&2 \times \mathop{\mathbb{E}}_{X,Y}[\text{PSMI}(X, Y) \mid \Delta = 1] \\
&= \mathop{\mathbb{E}}_{X,Y}[\text{PSMI}(X, Y) \mid \Delta = 1] + \mathop{\mathbb{E}}_{X,Y}[\text{PSMI}(X, 1 - Y) \mid \Delta = 1] \\
&= \int_{X,Y} \int_{\theta \sim \mathcal{U}(\mathbb{S}^d)} \left[\log \frac{p(\theta^T x, y)}{p(\theta^T x) p(y)} + \log \frac{p(\theta^T x, 1 - y)}{p(\theta^T x) p(1 - y)} \right] \mathrm{d}p(X, Y \mid \Delta = 1) \mathrm{d}p(\theta) \\
&= \int_{X,Y} \int_{\theta \sim \mathcal{U}(\mathbb{S}^d)} \left[\log \frac{p(\theta^T x \mid y) p(y) p(\theta^T x \mid 1 - y) p(1 - y)}{p(\theta^T x) p(y) p(\theta^T x) p(1 - y)} \right] \mathrm{d}p(X, Y \mid \Delta = 1) \mathrm{d}p(\theta) \\
&= \int_{X,Y} \int_{\theta \sim \mathcal{U}(\mathbb{S}^d)} \left[\log \frac{p(\theta^T x \mid y) p(\theta^T x \mid 1 - y)}{[p(\theta^T x \mid y) p(y) + p(\theta^T x \mid 1 - y) p(1 - y)]^2} \right] \mathrm{d}p(X, Y \mid \Delta = 1) \mathrm{d}p(\theta) \\
&= \int_{X,Y} \int_{\theta \sim \mathcal{U}(\mathbb{S}^d)} \left[\log \frac{p(\theta^T x \mid y) p(\theta^T x \mid 1 - y)}{\left[\frac{p(\theta^T x \mid y) + p(\theta^T x \mid 1 - y)}{2} \right]^2} \right] \mathrm{d}p(X, Y \mid \Delta = 1) \mathrm{d}p(\theta)
\end{aligned}$$

~~Now, we can apply the AM–GM inequality to $p(\theta^T x \mid y)$ and $p(\theta^T x \mid 1 - y)$. We find that the integrand in equation 14 is ≤ 0. Thus, the integral itself is ≤ 0, which proves equation~~ Consequently,

given $\Delta = 1$, X and Y are independent. We conclude that the expected value of PSMI is zero, which proves Equation 6.

$$\mathop{\mathbb{E}}_{X,Y}[\text{PSMI}(X,Y) \mid \Delta = 1] = \int_{X,Y} \int_{\theta \sim \mathcal{U}(\mathbb{S}^d)} \log \frac{p(\theta^T x, y)}{p(\theta^T x)p(y)} \mathrm{d}p(X, Y \mid \Delta = 1)\mathrm{d}p(\theta) \tag{12}$$

$$= \int_{X,Y} \int_{\theta \sim \mathcal{U}(\mathbb{S}^d)} \log \frac{p(\theta^T x)p(y)}{p(\theta^T x)p(y)} \mathrm{d}p(X, Y \mid \Delta = 1)\mathrm{d}p(\theta) \tag{13}$$

$$= 0 \tag{14}$$

Proof of ~~equation~~ Equation 5 First, we have:

$$\text{SMI}(X,Y) = \mathbb{E}[\text{PSMI}(X,Y)] \tag{15}$$

$$= \mathbb{E}[\text{PSMI}(X,Y) \mid \Delta = 0]p(\Delta = 0) + \mathbb{E}[\text{PSMI}(X,Y) \mid \Delta = 1]p(\Delta = 1) \tag{16}$$

Using ~~equation~~ Equation 6 that we have proved, we obtain:

$$\mathbb{E}[\text{PSMI}(X,Y) \mid \Delta = 0] > \text{SMI}(X,Y) \tag{17}$$

As a result, it is sufficient to demonstrate ~~equation~~ Equation 5 with $\text{SMI}(X,Y)$ instead of $\mathbb{E}[\text{PSMI}(X,Y) \mid \Delta = 0]$. To do this, we will apply Theorem 1 in (Wongso et al., 2023b). To do this, we search $(R_0, R_1, m_g, \nu) \in \mathbb{R}^4_{+,*}$ such that (X,Y) is (R_1, R_2, m_g, ν)-SSM separated with respect to Definition 3 in (Wongso et al., 2023b). Let $D = ||\mu_0 - \mu_1||$. Using μ_0 and μ_1 and the centers of the spheres, this means that (R_0, R_1, m_g, ν) should satisfy:

$$p(||X - \mu_0|| > R_0) = p(||X + \mu_1|| > R_1) = \nu \quad \text{and} \quad R_0 + R_1 + m_g = D \tag{18}$$

There are many values of (R_0, R_1, m_g, ν) which satisfy these conditions. When applying Theorem 1 in (Wongso et al., 2023b), these values give different lower bounds. Here is an algorithm to create a valid tuple (R_0, R_1, m_g, ν) given a hyperparameter $R \in]0, D/2[$.

1. Let S_0 (resp. S_1) be the sphere of center μ_0 (resp. μ_1) and radius R.
2. Let $\nu_0 = p(X \in S_0 \mid Y = 0)$ and $\nu_1 = p(X \in S_1 \mid Y = 1)$. Given the Gaussian assumptions we made in ~~equation~~ Equation 3, we have $\nu_0, \nu_1 \in]0, 1[$.
3. Let $i \in \{0, 1\}$ and $j = i - 1$ such that $\nu_i \geq \nu_j$. We fix $R_i = R$ and $\nu = \nu_i$.
4. We will now start with $R_j = R$ and decrease its value until ~~equation~~ Equation 18 is satisfied. Because X is a continuous random variable, the following function is continuous, decreasing, equal to 1 when $t = 0$, and because $\nu_j \leq \nu_i$, its value is $\leq \nu$ for $t = 1$:
$$t \in [0, 1] \mapsto p(||X - \mu_j|| > t \cdot R \mid Y = j) \tag{19}$$
5. As a consequence, due to the intermediate values theorem, there exists t_j in $]0, 1]$ such that $p(||X - \mu_j|| > t \cdot R \mid Y = j) = \nu$.
6. We set $R_j = t \cdot R$ and $m_g = D - R_0 - R_1$. Because $R_0, R_1 \leq R < D/2$, we have $m_g > 0$
7. Now, we can apply Theorem 1 in (Wongso et al., 2023b) :

$$\text{SMI}(X,Y) > (1 - H(\nu, 1 - \nu)) \times B_{\gamma(m_g, R_0, R_1)}\left(\frac{d-1}{2}, \frac{1}{2}\right) \tag{20}$$

Where:

- H is the entropy function $H(p_1, p_2) = -p_1 \log p1 - p_2 \log p_2$. We can easily prove that $(1 - H(\nu, 1-\nu)$ is convex on $]0, 1[$ and that its minimal value is > 0.
- $\gamma(m_g, R_0, R_1) = \frac{m_g}{m_g+R_0+R_1}\left(2 - \frac{m_g}{m_g+R_0+R_1}\right) = \frac{m_g}{D}\left(2 - \frac{m_g}{D}\right) \in]0, 1[$
- B is the incomplete beta function defined as follows. Because $\gamma(m_g, R_0, R_1) \in]0, 1[$, it is clear that its value is always > 0.

$$B_\gamma(a, b) = \int_0^\gamma t^{a-1}(1-t)^{b-1}\mathrm{d}t \tag{21}$$

This proves that $\mathrm{SMI}(X, Y) > 0$, which demonstrates ~~equation~~ Equation 6 and concludes the proof. □

Discussion on a better bound for ~~equation~~ Equation 5 The proof above provides a constructive algorithm to obtain $(R_0, R_1, m_g, \nu) \in \mathbb{R}^4_{+,*}$ such that (X, Y) is (R_1, R_2, m_g, ν)-SSM separated with respect to Definition 3 in (Wongso et al., 2023b). Depending on the hyperparameter $R \in]0, D/2[$, the bound is different. As a result, this hyperparameter can be optimized to find the better possible bound with this algorithm. We did not performed this optimization because it is not useful for the purpose of Theorem 1. Indeed, we only use this theorem to illustrate why we expect outliers in the hidden representations distribution to have a lower PSMI (see ~~section~~ Section 2.1).

C Implementation details

~~In this section we discuss how we implemented our experiments in practice. We~~ To help reproducing our results, we provide a GitHub repository containing the Python source code of our experiments, as well as the Bash and Slurm scripts to deploy them on a HPC cluster.[2] ~~In section~~ We also provide a PyPI package containing an automated estimator of PSMI that can be used in a wide range of scenarios.[3]

In this section we discuss how we implemented our experiments in practice. In Section C.1, we discuss how we adapted the baseline of Biderman et al. (2023) to classification, in Section C.2, we discuss how we implemented our measures of memorization, in ~~section~~ Section C.3 we elaborate on the implementation of our predictors~~, and in section ?? we explain how we repeated our experiment at minimal cost to ensure reproducibility~~.

C.1 Implementing our baseline

As explained in the introduction, the baseline of Biderman et al. (2023) is the only comparable method we are aware of. However, it is not directly applicable to our classification setting. Their method measures k-extractability (Carlini et al., 2021) on the partially trained model to predict memorization in the fully trained model. However, as explained in Section 1.1, extractability is rarely used to define memorization in a classification setting. Indeed, current extraction or reconstruction attacks against classification models are both more complex and less powerful than extraction attacks against generative models (Carlini et al., 2023). Consequently, we modified the baseline of Biderman et al. (2023) to suit our classification setting. While we still use memorization within the partially trained model to predict memorization in the final model, we replaced k-extractability by the vulnerability to LiRA attack.

The computational cost of this adapted baseline is significantly higher than that of the methods we evaluate, as it requires training the shadow models needed for LiRA attack. As a consequence, this baseline would not be suitable for practitioner within our threat model (see Section 1.2). Nevertheless, we compare our method to this baseline because it is the only comparable approach that assess the possibility of predicting memorization before the end of training.

[2] hidden_github_url_experiment_repo_for_review
[3] hidden_github_url_pypi_package_for_review

C.2 IMPLEMENTING MEMORIZATION MEASURES

The local version of LiRA, the global version, and counterfactual memorization all require a large number of shadow models (see details in ~~section~~ Section A). To minimize the computational cost of our experiments, for each dataset, we trained 100 shadow models on random splits containing half of the elements of the dataset. Each random split (and the model trained on it) is associated to a number between 0 and 99 (see `split_id` attribute in `training_cfg.py`) corresponding to the seed of the random split.

- **Local LiRA:** We select the model trained on random split 0 to be our target model, and use the 99 other models as the shadow models for the attack. In addition to the training cost, this requires one forward pass per shadow model on the training set of the target model (i.e. random split 0). Note that this is the setting used in the main body of the paper, so the PSMI is computed on this random split 0 and used to predict memorization for the model trained on it.
- **Global LiRA:** We attack each model with the 99 other models trained on different random splits, and measure the attack success rate on each sample x of the dataset. In addition to the training cost, this requires one forward pass per shadow model on *all* elements of the dataset.
- **Counterfactual memorization:** For each element x of the complete dataset, we separate the shadow models into two groups: the one that had x in the training set, and the others. Given that each random split contains half of the samples, these two groups have roughly the same size. We used them to compute counterfactual memorization (Zhang et al., 2023). In addition to the training cost, this requires one forward pass per shadow model on *all* elements of the dataset.

Note that in our GitHub repository, we use the term `dynamic` to describe local measures such as the local version of LiRA or the PSMI of the target model; and we use the term `static` to describe global measures on a population of models such as the global version of LiRA or counterfactual memorization. The training of these shadow model was by far the most expensive part of our experiments from a computational perspective. However, this operation can be parallelized on a many workers within an HPC cluster, because each shadow model is trained independently.

C.3 IMPLEMENTING PREDICTORS

Algorithm 1 in Section 2.3 explains how we use PSMI to predict memorization in the final model. This algorithm can be easily adapted to use other predictors instead of PSMI. For instance, Algorithm 2 illustrates how to use the loss as a predictor. Unlike PSMI, it does not require a hyperparameter to select a layer. However, as shown in Section 3.2, the choice of the last layer is robust across all empirical settings we evaluated, so this hyperparameter does not introduce additional complexity. Conversely, using the loss instead of PSMI requires an extra hyperparameter (denoted x in Algorithm 2) to define the proportion of samples to filter based on their loss values.

Algorithm 2 Using Loss to predict memorization

1: Interrupt training when the median training loss has decreased by at least **95%**.
2: Compute a forward pass for every sample to retrieve the **loss**.
3: Predict that every sample with **top** x**%** highest loss will be memorized.

We evaluated five possible metrics to predict memorization at the early stages of training. For the metrics that require the hidden states of the model (PSMI and Mahalanobis distance), we recall that the hidden state at layer k is defined as the representation of the last token (the one before the label) after layer k (see section 2.1).

- **PSMI.** We use algorithm 1 in (Wongso et al., 2023a) to estimate PSMI. We sample 2000 direction uniformly on the unit sphere. Indeed, we observed that the mutual information between random directions and the label has a mean of about $4.5 \cdot 10^{-3}$ and a standard deviation of about $5.5 \cdot 10^{-3}$. Thus, if we approximate these distributions by Gaussians, we

get a margin at 95% confidence interval of about $(1.96 \times 5.5 \cdot 10^{-3})/\sqrt{2000} \simeq 2.4 \cdot 10^{-4}$. This is about 20 times smaller than the mean, so we consider that our metric is stable enough with 2000 estimators.

- **Loss.** We directly use the cross-entropy loss of the model for the last token before the label. This metric was suggested by Leemann et al. (2024).
- **Logit Gap.** The logits are the outputs of the fully-connected layer applied to the last token, before the softmax. We define the logit gap as the difference between the logit of the correct prediction and the maximum logit of an incorrect prediction.
- **Early memorization.** We define early memorization as the natural logarithm of LiRA attack against the partially trained model.
- **Mahalanobis distance.** It is the Mahalanobis distance (Mahalanobis, 1936) of the hidden representation of a training sample to the distribution of hidden representation of the other training samples. To reduce computational costs, we first project every hidden states using a Principal Component Analysis (PCA) with a target dimension of 500. This metric was suggested by Azize & Basu (2024).
- **Our baseline: early memorization.** We define early memorization as the natural logarithm of LiRA attack against the partially trained model. See Appendix C.1.

C.4 Repeating our experiments on other shadow models

D Additional experiments

As explained in section C.2, we select random split 0 of the dataset to train our target model, and use the 99 other models as shadow models to measure memorization. As a result, our experiments can be repeated at minimal cost, by selecting another random split for the target model, and using the 99 other models as shadow models. With this procedure, we do not need to re-train any other model. We only need to compute a forward pass with each of the new shadow model on the new target random split (but we already had it because the global variant of LiRA already requires it), and to compute a forward pass with the new target model to compute PSMI and predict memorization.

D.1 TPR/FPR trade-offs for each setting at every checkpoint

We obtained similar results when repeating our experiments on other random splits, confirming the reliability of our empirical findings.

E Additional plots

We provide four additional plots: Figure **??**: histograms of memorization for various checkpoints during training, for each of our experimental settings. See discussion on figure **??**. Figure **??**: impact of the quantile used to define memorization. See discussion on figure **??**. Figure **??**: impact of the checkpoint used for prediction. See discussion on figure 3a. Figure **??**: TPR

D.1 Additional results on the dynamics of training

We always interrupt training when the median training loss has decreased by 95%, and measure ground truth memorization after 1 epoch of training (see Section 3). To validate this choice, we conducted the experiments described in Section 3.2. Figure 8 presents additional plots for experimental settings not discussed in that section. These results confirm that memorization can be predicted early in the training pipeline and that memorized samples have not yet been memorized at that point.

Special case of ARC/Mistral Table 1 presents the decrease of the median training loss relative to epoch 0 throughout training. We saved models every 0.2 epoch to analyze them and measure their performance. We observe that for ARC/Mistral, the median training loss has decreased by 93.724% at epoch 0.2, which is close to 95%. Conversely, by epoch 0.4, the median training loss has decreased

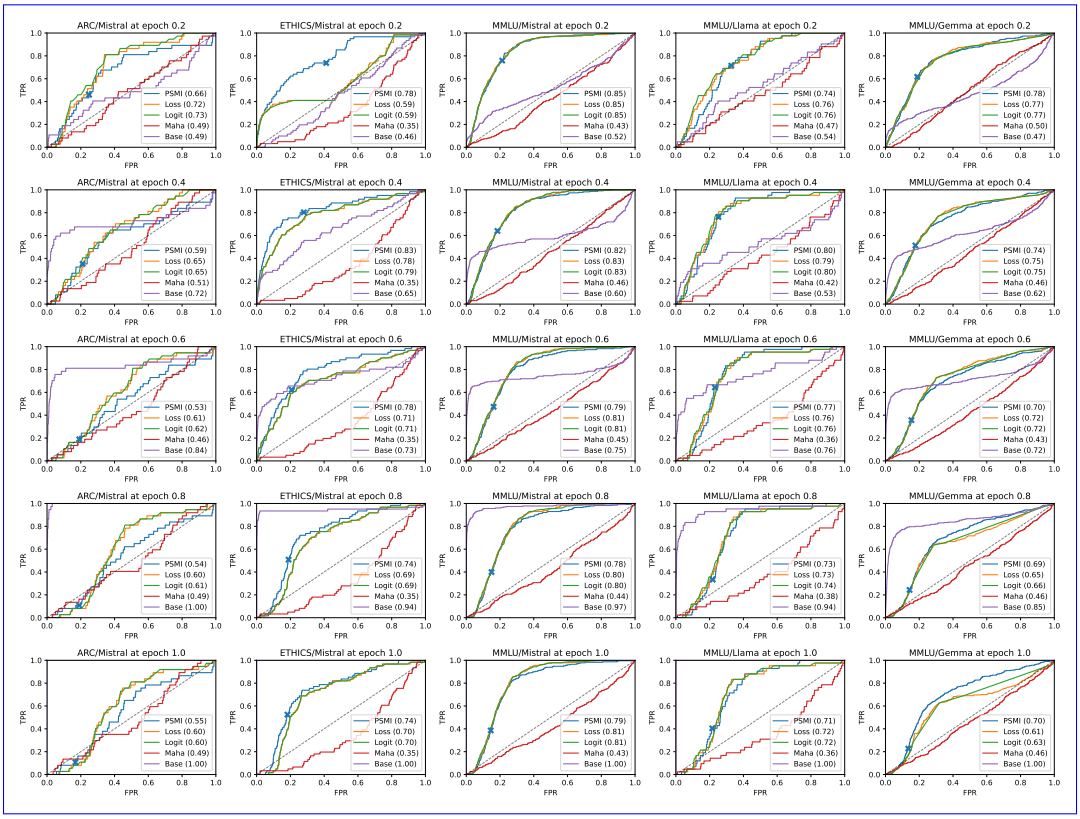

Figure 7: TPR/FPR trade-offs for each setting at every checkpoint. The number in parentheses corresponds to the AUC of the curve. The blue cross indicates the result using the default hyperparameters of Algorithm 1. The AUC of the baseline ("Base") converges to 1.0 at epoch 1.0 because, at that stage, the baseline is the same as what we are trying to predict. We remind that practitioners within our threat model do not have the resources to compute the baseline and instead attempt to approximate it using other metrics early in the training pipeline.

	Epoch 0	Epoch 0.2	Epoch 0.4	Epoch 0.6	Epoch 0.8	Epoch 1
ARC/~~FPR trade-offs at each checkpoint, for every experimental setting. See discussion on figure 2b.~~ Mistral	0.000%	93.724%	98.015%	99.397%	98.907%	99.222%
ETHICS/Mistral	0.000%	86.036%	95.198%	98.985%	99.665%	99.739%
MMLU/Mistral	0.000%	98.967%	99.776%	99.916%	99.916%	99.895%
MMLU/Llama	0.000%	91.674%	98.186%	99.329%	99.336%	99.267%
MMLU/Gemma	0.000%	99.543%	99.606%	99.855%	99.980%	99.979%

Table 1: Decrease in the median training loss relative to epoch 0 throughout training.

by significantly more than 95%. This is why, for that setting, we predict memorization at epoch 0.2, the checkpoint where the decrease is closest to 95%. For the other settings, as indicated in Section 3, we predict memorization at the first checkpoint where the median training loss has decreased by at least 95%.

D.2 Histograms of memorization throughout training

D.3 Additional results on the impact of the memorization threshold

D.4 Ablation study on the layers for Mahalanobis distance

Similar to the approach in Section 3.2 and Figure 4b, we conducted an ablation study on the layers for Mahalanobis distance (see Figure 11). These results were used in the other figures to ensure that the Mahalanobis distance is computed at the layer that maximizes the resulting AUC value.

D.5 ADDITIONAL RESULTS WITH CIFAR-10

Figure 12 presents additional results obtained by applying our method as-is to a wide residual network trained from scratch on CIFAR-10. We vary the threshold applied to log-LiRA to define memorized samples. We observe that our method becomes increasingly effective as the samples to be detected become more highly memorized. It converges towards the experiment on the right of the figure, where memorized samples are defined as the canaries crafted by (Aerni et al., 2024) to mimic the most vulnerable samples.

For these experiments, the model was trained for 300 epochs, and we interrupted training after 4 epochs, when the median training loss had decreased by 95%.

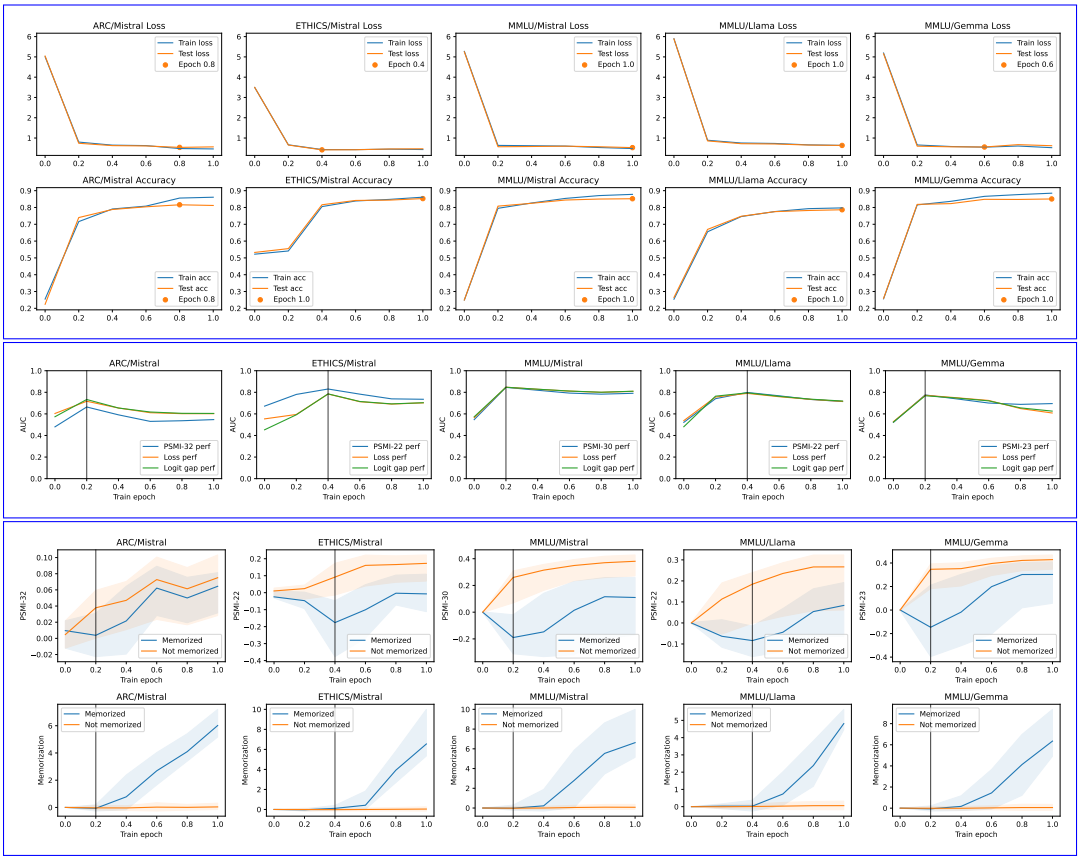

Figure 8: Additional results related to the dynamics of training and the appropriate moment to interrupt training. **First row:** Training loss, testing loss, and epoch of the best testing loss for each experimental setting. **Second row:** Training accuracy, testing accuracy, and epoch of the best testing accuracy for each experimental setting. **Third row:** AUC of PSMI, Loss and Logit Gap for predicting memorization. The vertical line indicates the point at which training loss has decreased by 95%, marking the moment when training is stopped to predict memorization. **Fourth row:** The solid line shows the median PSMI for samples that will be memorized or not within the fully trained model. The shaded area represents the 25%-75% quantiles. PSMI is measured at the layer that obtained the highest AUC. **Fifth row:** Similar representation for the memorization within the partially trained model.

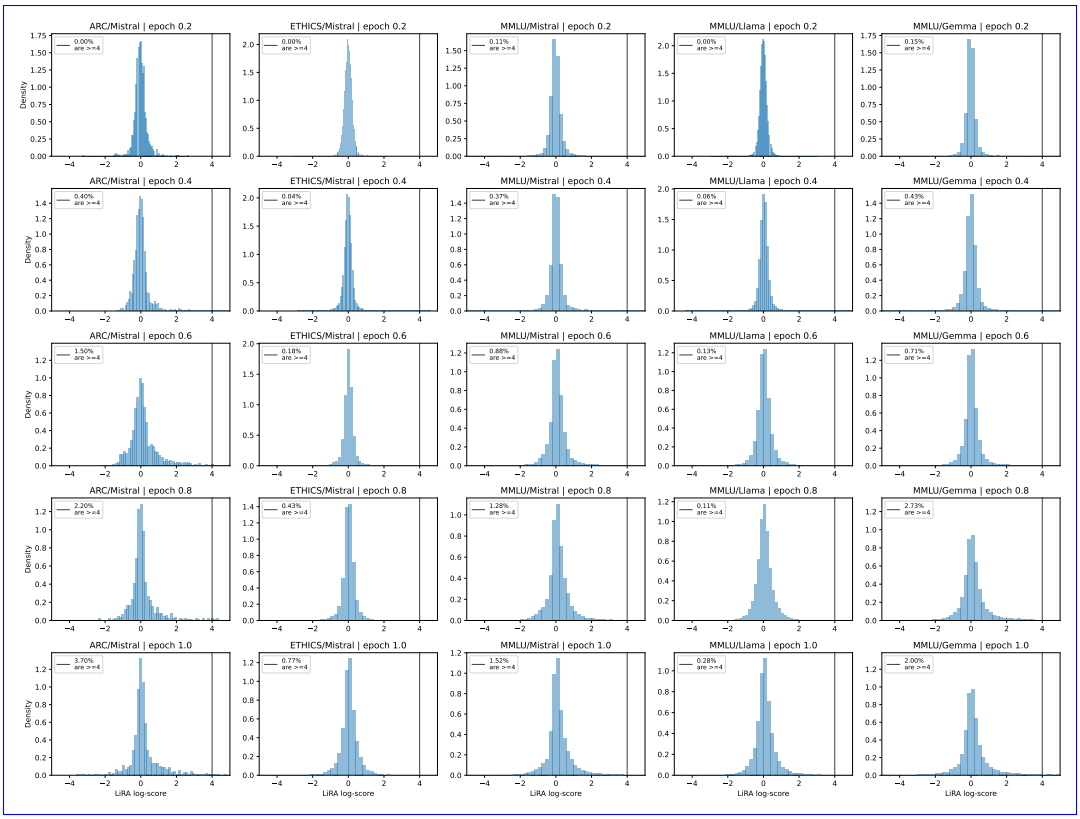

Figure 9: Histograms of memorization throughout training. The legend displays the proportion of samples with log-LiRA ≥ 4, which is the threshold used to define memorization in all figures unless otherwise specified.

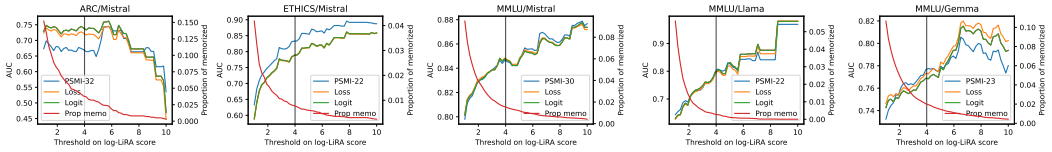

Figure 10: Impact of the threshold used to define "memorized" and "non memorized" samples. The vertical bar indicates the default threshold log-LiRA = 4.

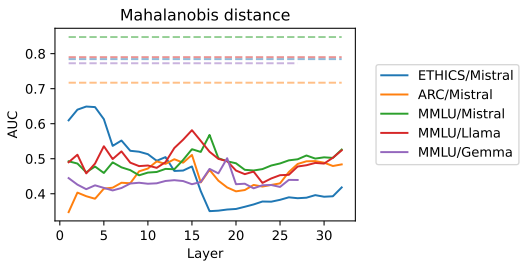

Figure 11: Impact of the choice of layer on the AUC using the Mahalanobis distance. The dashed lines represent the AUC with the loss, which is independent of the layer.

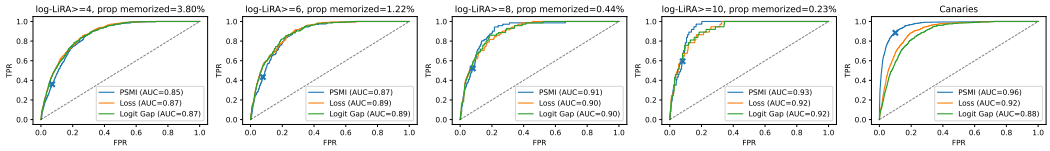

Figure 12: ~~Histograms~~ Predicting memorized samples on a WRN16-4 (Zagoruyko & Komodakis, 2016) trained from scratch on CIFAR-10 using the framework of Aerni et al. (2024). In the first four graphs, we vary the threshold applied to log-LiRA ~~scores at different checkpoints~~to define memorized samples. The ~~green lines indicate~~ title displays the ~~10% quantile~~proportion of memorized samples in the fully trained model using this definition. The blue cross marks the performance of the default hyperparameters from Algorithm 1. The last graph presents the same experiment, ~~and~~ where memorized samples are defined as the ~~orange line represents~~ canaries inserted by Aerni et al. (2024) to mimic the ~~Gaussian kernel density estimation~~most vulnerable samples in the training set.

~~Impact of the quantile used to define memorization, as in figure ??. We observe that is is always easier to predict samples that are strongly memorized, i.e. the ones in the low quantiles such as top-5% or top-10%. We recall that the 10% quantile is the default one used for the other plots. Impact of the checkpoint used to predict memorization, as in figure 3a. The vertical line represents the first checkpoint where the median training loss has decreased by 95% (epoch 0.2 for MMLU/Mistral and MMLU/Gemma; epoch 0.4 for the others). We observe that the predictors are not very efficient before the vertical line, which is consistent with what is discussed in section 3.2. TPR / FPR trade-offs in each of our experimental settings. Each row corresponds to a different checkpoint used to predict memorization. The cross corresponds to the default method presented in algorithm 1, using the last layer. The two percentage in the corresponding legend are the FPR and TPR, respectively. The lines represents the TPR / FPR trade-offs when optimizing the hyperparameters, as in figure 2b. The numbers in the legend are the FPR@TPR=0.75 scores. Memorization is always measured at epoch 10.~~